arXiv:1512.03066v1 [astro-ph.HE] 9 Dec 2015

Theory and Applications of Non-Relativistic and Relativistic Turbulent Reconnection

A. Lazarian, G. Kowal, M. Takamoto, E. M. de Gouveia Dal Pino, and J. Cho

Abstract Realistic astrophysical environments are turbulent due to the extremely high Reynolds numbers of the flows. Therefore, the theories of reconnection intended for describing astrophysical reconnection should not ignore the effects of turbulence on magnetic reconnection. Turbulence is known to change the nature of many physical processes dramatically and in this review we claim that magnetic reconnection is not an exception. We stress that not only astrophysical turbulence is ubiquitous, but also magnetic reconnection itself induces turbulence. Thus turbulence must be accounted for in any realistic astrophysical reconnection setup. We argue that due to the similarities of MHD turbulence in relativistic and non-relativistic cases the theory of magnetic reconnection developed for the non-relativistic case can be extended to the relativistic case and we provide numerical simulations that support this conjecture. We also provide quantitative comparisons of the theoretical predictions and results of numerical experiments, including the situations when turbulent reconnection is self-driven, i.e. the turbulence

A. Lazarian
Department of Astronomy, University of Wisconsin, Madison, Wisconsin, USA, e-mail: lazarian@astro.wisc.edu

G. Kowal
Escola de Artes, Ciências e Humanidades, Universidade de São Paulo, São Paulo, SP, Brazil, e-mail: grzegorz.kowal@usp.br

M. Takamoto
Department of Earth and Planetary Science, The University of Tokyo, Tokyo, Japan, e-mail: mtakamoto@eps.s.u-tokyo.ac.jp

E. M. de Gouveia Dal Pino
Instituto de Astronomia, Geofísica e Ciencias Atmosfericas, Universidade de Sao Paulo, São Paulo, SP, Brazil, e-mail: dalpino@astro.iag.usp.br

J. Cho
Department of Astronomy and Space Science, Chungnam National University, Daejeon, Korea, e-mail: jcho@cnu.ac.kr

in the system is generated by the reconnection process itself. We show how turbulent reconnection entails the violation of magnetic flux freezing, the conclusion that has really far reaching consequences for many realistically turbulent astrophysical environments. In addition, we consider observational testing of turbulent reconnection as well as numerous implications of the theory. The former includes the Sun and solar wind reconnection, while the latter include the process of reconnection diffusion induced by turbulent reconnection, the acceleration of energetic particles, bursts of turbulent reconnection related to black hole sources as well as gamma ray bursts. Finally, we explain why turbulent reconnection cannot be explained by turbulent resistivity or derived through the mean field approach. We also argue that the tearing reconnection transfers to fully turbulent reconnection in 3D astrophysically relevant settings with realistically high Reynolds numbers.

Key words: reconnection, turbulence, particle acceleration, gamma ray bursts, stellar activity

1 Problem of reconnection as we see it

This is a chapter that deals with magnetic reconnection in astrophysical environments that are generically turbulent. We discuss how turbulence makes reconnection fast and what this means for many astrophysical systems.

This is a contribution to the book on magnetic reconnection and therefore it is not particularly productive to repeat that magnetic reconnection is important for variety of processes from solar flares to gamma ray bursts. What we would like to stress here is that magnetic reconnection is not some exotic process that may be taking place occasionally in astrophysical environments, but it is bread and butter of most processes taking place in magnetized plasmas. The key to understanding of omnipresence of magnetic reconnection is the ubiquity of turbulence in astrophysical environments.

Turbulence is a feature of high Reynolds number flows and most of magnetized flows have extremely high Reynolds numbers. We show that even if the initial astrophysical setup is not turbulent or "not sufficiently turbulent", the development of reconnection, e.g. outflow, is bound to transfer the process of reconnection to fully turbulent regime. Therefore we view the laminar models with plasma instabilities, e.g. tearing instability, as transient states to the fully turbulent reconnection.

What is the speed of reconnection? It is important to stress that turbulent reconnection can address the apparent dichotomy suggested by observations, e.g. reconnection is sometimes fast and sometimes slow. The theory of turbulent reconnection relates this to the dependence of magnetic reconnection rate on the level of turbulence in the system. As the intensity of turbulence changes, the reconnection rate also changes.

As we will discuss in the review, the theory of turbulent reconnection predicts reconnection rates that do not depend on the details of plasma microphysics, but only on the level of MHD turbulence. The plasma physics related to the local reconnection events may still be important at small scales e.g. for the acceleration of particles from the thermal pool. At the same time, for understanding of particle acceleration at large energies we will claim that the MHD description of turbulent reconnection is sufficient. We note, however, that the turbulent reconnection theory that we describe in the review is based on MHD and therefore it is not applicable to the Earth magnetosphere where the current sheets are comparable to the ion inertial scale.

The theory of turbulent reconnection has been covered in a number of reviews that include Lazarian et al (2015a,b); Browning and Lazarian (2013). In a review by Karimabadi and Lazarian (2013) there was also an attempt to present side by side both the theories of turbulent reconnection based on plasma turbulence and on MHD approach, that we discuss here. We warn our readers, however, that the statement in the latter review that the MHD approach has problems with describing reconnection events in Solar wind was shown to be incorrect in (Lalescu et al, 2015).

Within the present review we also discuss the implications of turbulent reconnection, the latter study becoming more important as the interconnection between turbulence and astrophysical reconnection is appearing more evident to the community. However, in terms of implications, we are just scratching the surface of a very rich subject. Some implications are rather dramatic and has far reaching consequences. For instance, it is generally believed that magnetic fields embedded in a highly conductive fluid retain their topology for all time due to the magnetic fields being frozen-in (Alfvén, 1943; Parker, 1979). This concept of frozen-in magnetic fields is at the foundation of many theories, e.g. of the theory of star formation in magnetized interstellar medium. At the same time, in the review we discuss that this concept is not correct in the presence of turbulence. As a result, serious revisions are necessary for the theoretical description of a large number of astrophysical systems.

In what follows we briefly discuss modern ideas on non-relativistic and relativistic MHD turbulence in §2 and §3 respectively, introduce the basic concepts of turbulent non-relativistic reconnection theory in §4, provide numerical testing of turbulent reconnection in §5. In §6 we discuss how non-relativistic turbulent reconnection theory can be generalized for the case of relativistic reconnection and provide numerical testing of the idea, while §7 deals with the case of turbulent reconnection where turbulence is injected by the reconnection process itself. The observational testing of turbulent reconnection is discussed in §8 and the implications of the theory of turbulent reconnection are summarized in §9. A comparison of turbulent reconnection to other popular ideas can be found in §10 and the final remarks are given in §11. There we also discuss the relation of the material in this chapter to that in other chapters of the book.

2 Non-Relativistic MHD turbulence

Non-relativistic MHD turbulence is the best explored case with a lot of observational and numerical data available to test the theory.

2.1 Astrophysical turbulence: expectations and evidence

Magnetized astrophysical fluids have huge Reynolds numbers $Re \equiv LV/\nu$ as magnetic field limits the diffusion of charged particles perpendicular to its local direction making viscosity ν small[1] while the scales of the flow L are astrophysically huge. High Re number flows are prey to numerous linear and finite-amplitude instabilities, from which turbulent motions readily develop. The plasma turbulence is can be driven by external energy sources, such as supernovae in the ISM (Norman and Ferrara, 1996; Ferrière, 2001), merger events and active galactic nuclei outflows in the intracluster medium (ICM) (Subramanian et al, 2006; Enßlin and Vogt, 2006; Chandran, 2005), and baroclinic forcing behind shock waves in interstellar clouds. In other cases, the turbulence is spontaneous, with available energy released by a rich array of instabilities, such as magneto-rotational instability (MRI) in accretion disks (Balbus and Hawley, 1998), kink instability of twisted flux tubes in the solar corona (Galsgaard and Nordlund, 1997; Gerrard and Hood, 2003), etc. Finally, as we discuss in the review, magnetic reconnection can also be a source of turbulence.

Observations confirm that astrophysical environments are indeed turbulent. The spectrum of electron density fluctuations in the Milky Way is presented in Figure 1, but similar examples are discussed in Leamon et al (1998), Bale et al (2005) for solar wind, and Vogt and Enßlin (2005) for the intracluster medium. As new techniques for studying turbulence are being applied to observational data, the evidence of the turbulent nature of astrophysical media becomes really undeniable. For instance, the Velocity Channel Analysis (VCA) and Velocity Coordinate Spectrum (VCS) techniques (Lazarian and Pogosyan, 2000, 2004, 2006) provided unique insight into the velocity spectra of turbulence in molecular clouds (see Padoan et al, 2006, 2010), galactic and extragalactic atomic hydrogen (Stanimirović and Lazarian (2001); Chepurnov et al (2010, 2015), see also the review by Lazarian (2009), where a compilation of velocity and density spectra obtained with contemporary HI and

[1] In addition, the mean free path of particles can also be constrained by the instabilities developed in turbulent plasmas below the scale determined by Coulomb collisions (see Schekochihin et al, 2009; Lazarian and Beresnyak, 2006; Brunetti and Lazarian, 2011). The resulting scattering arising from the ion interactions with the perturbed magnetic field ensures that compressible motions are much more resilient to the collisionless damping compared to the textbook results obtained with the Spitzer cross sections for ion collisions.

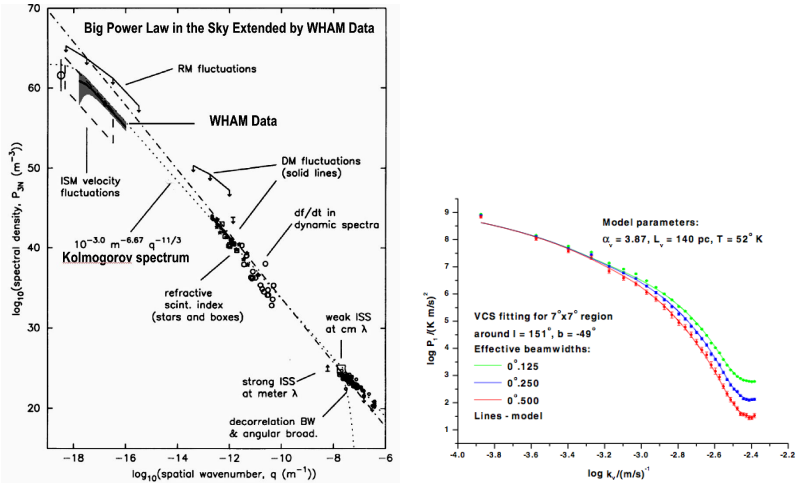

Fig. 1 *Left Panel* Big power law in the sky from Armstrong et al (1995) extended to scale of parsecs using the Wisconsin H-Alpha Mapper (WHAM) data. Reproduced from Chepurnov and Lazarian (2010) by permission of the AAS. *Right Panel*. Properties of turbulence in HI obtained with VCS techniques. Reproduced from Chepurnov et al (2010) by permission of the AAS.

CO data is presented). We expect new flow of information on magnetic field spectra to come from the new techniques that treat synchrotron fluctuations (Lazarian and Pogosyan, 2012).

2.2 Theory of weak and strong MHD turbulence

MHD theory is applicable to astrophysical plasmas at sufficiently large scales and for many astrophysical situations the Alfvénic turbulence, which is the most important for turbulent reconnection and is applicable at the scales substantially larger than the ion gyroradius ρ_i (see a discussion in Eyink et al, 2011; Lazarian et al, 2015a).

The history of the theory of MHD turbulence can be traced back to the pioneering studies by Iroshnikov (1964) and Kraichnan (1965). A good account for the state of the field could be found in Biskamp (2003). Usually turbulence is subdivided into weak and strong regimes, depending on the strength of nonlinear interaction. While weak MHD turbulence allows for analytical perturbative treatment (Ng and Bhattacharjee, 1996; Galtier et al, 2002; Chandran, 2005), the progress in understanding strong turbulence came primarily from phenomenological and closure models that were tested by comparison with results of numerical simulations. Important theoretical works on strong MHD turbulence include Montgomery and Turner (1981), Matthaeus et al (1983),

Shebalin et al (1983), and Higdon (1984). Those clarified the anisotropic nature of the energy cascade and paved the way for further advancement in the field. The study by Goldreich and Sridhar (1995) identified the balance between perturbations parallel and perpendicular to the local direction of magnetic field, i.e., "critical balance", as the key component of dynamics in strong magnetic turbulence. For detailed recent reviews on MHD turbulence, see Brandenburg and Lazarian (2013) and Beresnyak and Lazarian (2015). Below we provide a simplified derivation of the Alfvénic turbulence scaling that we employ later to understand turbulent reconnection (see also Cho et al, 2003). Other ways of obtaining the same relations may be found in e.g. Goldreich and Sridhar (1995), Lazarian and Vishniac (1999), and Galtier et al (2000). Other fundamental modes, i.e. slow and fast modes are of relatively marginal importance for the theory of turbulent reconnection and we do not discuss them in the review[2].

If all the Alfvénic wave packets are moving in one direction, then they are stable to nonlinear order. Therefore, in order to initiate turbulence, there must be opposite-traveling wave packets of similar dimensions and the energy cascade occurs only when they collide. It is also natural to assume that the wave packets are anisotropic and therefore to distinguish between the parallel $l_\parallel$ and the perpendicular $l_\perp$ scales of the wave-packets. The change of energy per collision is

$$\Delta E \sim (du^2/dt)\Delta t \sim \mathbf{u}_l \cdot \dot{\mathbf{u}}_l \Delta t \sim (u_l^3/l_\perp)(l_\parallel/V_A), \quad (1)$$

where we take into account that Alfvénic motions perpendicular to magnetic field providing $\dot{\mathbf{u}}_l \sim u_l^2/l_\perp$, while the time of interactions is determined by the time of wave packets interacting with each other, i.e. $\Delta t \sim l_\parallel/V_A$, where V_A is the Alfvén velocity.

The fractional energy change per collision is the ratio of ΔE to E,

$$\zeta_l \equiv \frac{\Delta E}{u_l^2} \sim \frac{u_l l_\parallel}{V_A l_\perp}, \quad (2)$$

which characterizes the strength of the nonlinear interaction. The cascading is a random walk process in such a description with

$$t_{cas} \sim \zeta_l^{-2} \Delta t. \quad (3)$$

The Alfvénic 3-wave resonant interactions are characterized by

$$\mathbf{k}_1 + \mathbf{k}_2 = \mathbf{k}_3, \quad (4)$$

$$\omega_1 + \omega_2 = \omega_3, \quad (5)$$

[2] These modes may play decisive role other processes, e.g. for cosmic ray scattering (see Yan & Lazarian 2002, 2003a), acceleration of charged dust (see Yan & Lazarian 2003b), star formation (see McKee & Ostriker 2007).

where $\mathbf{k}$'s are wavevectors and ω's are wave frequencies. The first condition is a statement of wave momentum conservation and the second is a statement of energy conservation. Alfvén waves satisfy the dispersion relation: $\omega = V_A|k_\parallel|$, where $k_\parallel$ is the component of wavevector parallel to the background magnetic field. Since only opposite-traveling wave packets interact, $\mathbf{k}_1$ and $\mathbf{k}_2$ must have opposite signs, which formally means that the cascade is possible only in the perpendicular direction.

In fact, the energy relation is subject to the wave uncertainty principle, which means that the ambiguity of the order $\delta\omega \sim 1/t_{cas}$ is acceptable. When ζ_l is small, $\delta\omega \ll \omega$ and the energy transfer is happening mostly perpendicular to the *local* direction of magnetic field. As a result of such a cascade the parallel scale $l_\parallel$ is preserved, while the perpendicular scale $l_\perp$ decreases. This is the case of *weak Alfvénic turbulence*. In incompressible turbulence the energy flux is

$$\epsilon = u_l^2/t_{cas} \approx \frac{u_l^4}{V_A^2 \Delta t (l_\perp/l_\parallel)^2} = const \qquad (6)$$

where Eqs. (3) and (2) are used. Taking into account that $l_\parallel$ is constant, it is easy to see that Eq. (6) provides $u_l \sim l_\perp^{1/2}$ which in terms of energy spectrum of weak turbulence provides the relation

$$E_{k,weak} \sim k_\perp^{-2}, \qquad (7)$$

where the relation $kE(k) \sim u_k^2$ is used. Eq. (7) was obtained on the basis of similar arguments in Lazarian and Vishniac (1999, henceforth LV99) and later on the basis of a rigorous treatment of weak turbulence in Galtier et al (2000). Note that $k_\parallel$ stays constant in the weak cascade.

Note, that the weak turbulence regime should have a limited inertial range. Indeed, as $k_\perp \sim l_\perp^{-1}$ increases, the energy change per collision ζ_l increases, the cascading time t_{cas} decreases. This makes the uncertainty in the wave frequency $\delta\omega \sim 1/t_{cas}$ comparable to wave frequency ω when ζ_l approaches unity. Naturally, one expects the nature of the cascade to change. Indeed, the cascading cannot happen in less than one wave period and therefore the cascading rate cannot increase further. Similarly with $\delta\omega \sim \omega$ the constraints given by Eq. (5) cannot prevent the decrease of the parallel length of wave packets $l_\parallel$. This signifies the advent of a regime of *strong Alfvénic turbulence*. The corresponding theory was formulated for the turbulent injection velocity $u_L = V_A$ by Goldreich and Sridhar (1995, henceforth GS95) and was generalized for subAlfvénic and superAlfvénic injection velocities in LV99 and Lazarian (2006), respectively. Below we follow LV99 in order to obtain the relations for strong MHD turbulence with subAlfvénic energy injection. This type of turbulence is the most important in the context of turbulent reconnection.

As we explained above the change of the turbulence regime happens when $\zeta_l \sim 1$, which in terms of the parameters of the interacting wave packets means that

$$u_l/l_\perp \sim V_A/l_\parallel, \tag{8}$$

which manifests the famous GS95 *critical balance*. This expression was originally formulated using not scales of the eddies, but wavevectors $k_\perp$ and $k_\parallel$ as the GS95 discussion did not include the fundamental concept of *local* magnetic field direction. Indeed, the weak turbulence theory can be formulated in terms of mean magnetic field, as the distortions introduced by turbulence in terms of direction are marginal due to the marginal change of $l_\parallel$. In the strong turbulence the distinction between the mean direction of magnetic field and the local direction of the field that a wave packet is moving along may be significant. This is especially obvious in the case of transAlfvénic and super-Alfvénic turbulence when the local direction of magnetic field may poorly correlate with the direction of the mean magnetic field in the volume. As a result no universal relations exist in the frame of the mean magnetic field and therefore in the global frame given by wavevectors k. The understanding of the importance of the local magnetic frame for the GS95 theory was introduced and elaborated in the later publications (LV99; Cho and Vishniac, 2000; Maron and Goldreich, 2001; Cho et al, 2002a).

The turbulence is injected isotropically at scale L_i with the the velocity $u_L < V_A$ and the cascading of energy follows the weak turbulence cascade u_L^2/t_{cas}, which for the weak cascading rate gives $u_L^4/(L_i V_A)$. Starting with the scale corresponding to $\zeta_l = 1$, i.e. at the perpendicular scale

$$l_{trans} \sim L_i (u_L/V_A)^2 \equiv L_i M_A^2, \quad M_A < 1, \tag{9}$$

where $M_A = u_L/V_A < 1$ is the Alfvénic Mach number[3]. The turbulence becomes strong and cascades over one wave period, namely, $l_\parallel/V_A$. The cascading of turbulent energy is $u_l^3/l_\perp$, which is similar to Kolmogorov cascade in the direction perpendicular to the local direction of magnetic field. Due to the conservation of energy in the cascade the weak and strong turbulence energy flows should be the same which gives the scaling relations in LV99

$$\ell_\parallel \approx L_i \left(\frac{\ell_\perp}{L_i}\right)^{2/3} M_A^{-4/3}, \tag{10}$$

$$\delta u_\ell \approx u_L \left(\frac{\ell_\perp}{L_i}\right)^{1/3} M_A^{1/3}. \tag{11}$$

[3] Thus, weak turbulence has a limited, i.e. $[L_i, L_i M_A^2]$ inertial range and at small scales it transits into the regime of strong turbulence. We should stress that weak and strong are not the characteristics of the amplitude of turbulent perturbations, but the strength of non-linear interactions (see more discussion in Cho et al (2003)) and small scale Alfvénic perturbations can correspond to a strong Alfvénic cascade.

Those relations give the GS95 scaling for $M_A \equiv 1$. These are equations that we will use further to derive the magnetic reconnection rate.

When the measurements are done in the global system of reference, the turbulence scaling is dominated by perpendicular fluctuations containing most of energy, and therefore using Eq. (11) with $kE(k) \sim u_k^2$ one can get $E(k) \sim k^{-5/3}$, which coincides with the Kolmogorov scaling. One can intuitively understand this result assuming that eddies freely evolve in the direction perpendicular to magnetic field.

Finally, we want to point out that the isotropic driving of MHD turbulence is somewhat idealized. For instance, when turbulence is driven by magnetic reconnection, magnetic field lines are not straight on the injection scale and therefore the weak cascade ideas are not applicable. This is an important point for understanding Solar flares and similar reconnection phenomena.

2.3 Controversy related to GS95 model

Testing of GS95 turbulence numerically presented a challenging task. The measurements of the spectral slope in MHD simulations (see Maron and Goldreich, 2001) were better fitted by the spectrum $\sim k^{-3/2}$ rather than GS95 prediction of $k^{-5/3}$. This resulted in theoretical attempts to explain the measured slope by Boldyrev (2005, 2006). Another explanation of the slope difference was suggested in Beresnyak and Lazarian (2010). It was based on the conjecture that the MHD turbulence is less local compared to hydrodynamic turbulence and therefore low resolution numerical simulations were not measuring the actual slope of the turbulence, but the slope distorted by the bottleneck effect. The latter is generally accepted to be a genuine feature of turbulence and is attributed to the partial suppression of non-linear turbulent interactions under the influence of viscous dissipation. Studied extensively for hydrodynamics the bottleneck effect reveals itself as a pile-up of kinetic energy near the wave number of maximum dissipation (see Sytine et al, 2000; Dobler et al, 2003). With the limited inertial range of existing numerical simulations, the bottleneck effect may strongly interfere with the attempts to measure the actual turbulence spectrum. The locality of turbulence determines whether the bottleneck produces a localized or more extended bump of the turbulence spectrum. In the latter case the low resolution numerical simulations may be affected by the bottleneck effect for the whole range of wave numbers in the simulation and the distorted spectrum can be mistaken for an inertial range. A smooth extended bottleneck is expected for MHD turbulence being less local compared to its hydrodynamic counterpart. This feature of MHD turbulence was termed by Beresnyak & Lazarian "diffuse locality" (see Beresnyak and Lazarian, 2010). This effect is illustrated by Figure 2.

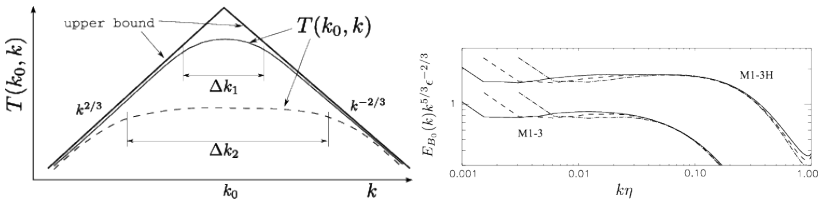

Fig. 2 *Left Panel* Illustration of "diffuse locality" of MHD turbulence. The upper bounds for the energy transfer window could be consistent with both rather "local" transfer (upper solid curve) or "non-local" and "diffuse-local" transfer (lower dashed curve). Reproduced from Beresnyak and Lazarian (2010) by permission of the AAS. *Right Panel.* Spectrum of MHD turbulence in high resolution simulations is consistent with GS95 predictions. Reproduced from Beresnyak (2015) by permission of the AAS.

All in all, the bottleneck is a physical effect and the absence of it in the low resolution MHD simulations is suggestive that the measured spectral slope is not the actual slope of the turbulent energy. In fact, the bottleneck effect has tricked researchers earlier. For instance, the initial compressible simulations suggested the spectral index of high Mach number hydrodynamic turbulence to be $-5/3$, which prompted theoretical attempts to explain this (e.g. Boldyrev, 2002). However, further high resolution research (Kritsuk et al, 2007) revealed that the flattering of the spectrum observed was the result of a bottleneck effect, which is more extended in compressible than in incompressible fluids. Similarly, we believe that the simulations that reported the spectral slope of $-3/2$ for the MHD turbulence (Maron and Goldreich, 2001; Müller and Grappin, 2005; Mason et al, 2006, 2008; Perez et al, 2012) are affected by the bottleneck effect. This conclusion is supported by the study of scaling properties of turbulence with high numerical resolution in Beresnyak (2014). This study shows that the Reynolds number's dependence of the dissipation scale is not fulfilled with the $-3/2$ spectral slope.

We believe that the new higher resolution simulations (see Beresnyak, 2013, 2014) resolve the controversy and, indeed, the putative $k^{-3/2}$ spectrum is the result of the bottleneck. However, whether the slope is $-3/2$ or $-5/3$ has only marginal impact on the theory of turbulent reconnection. A discussion of turbulent reconnection for an arbitrary spectral index and arbitrary anisotropy can be found in LV99.

2.4 Compressible MHD turbulence

As we discuss later, the Alfvénic mode is the most important mode for turbulent reconnection. Therefore we do not dwell upon compressible MHD turbulence. In fact, it is important for us to be able to consider Alfvénic perturbations in compressible turbulence. In a sense, in view of our further

discussion we are only interested in (1) whether the treatment of magnetic reconnection in terms of Alfvénic turbulence is adequate in the presence of fluid compressibility and (2) what portion of energy of driving is going into the Alfvénic component of turbulence.

Original ideas about how Alfvénic modes can interact with other fundamental modes, i.e. slow and fast modes, can be traced back to GS95. They were elaborated further in Lithwick and Goldreich (2001). A numerical and theoretical study of the modes was then performed in Cho and Lazarian (2002, 2003) and Kowal and Lazarian (2010). These studies answer positively the question (1), i.e. they show that turbulent Alfvénic mode preserves its identity and forms an independent Alfvénic cascade even in compressible fluid (see more in Cho and Lazarian, 2002, 2003). They also address the question (2), i.e. they quantify how much energy is transferred to compressible motions in MHD turbulence. The effects of compressibility have been extensively studied in Kowal et al (2007) and scaling relations has been tested in Kowal and Lazarian (2007). A detailed discussion of the effects of compressibility on MHD turbulence can be found in a review by Beresnyak and Lazarian (2015).

3 Relativistic MHD Turbulence

Some astrophysical fluids involve relativistic motions. In recent years, interest on MHD turbulence in relativistic fluids has been growing. Can the ideas of GS95 turbulence be transferred to relativistic fluids? This is the issue that has been addressed by recent research. Due to advances in numerical techniques, it is now possible to numerically investigate fully relativistic MHD turbulence (e.g. Zrake and MacFadyen, 2012).

3.1 Relativistic force-free MHD turbulence

Due to its numerical and theoretical simplicity, MHD turbulence in relativistic force-free regime has been studied first. Relativistic force-free formalism can be used for a system, such as the magnetosphere of a pulsar or a black hole, in which the magnetic energy density is much larger than that of matter. In this case, the Alfvén speed approaches the speed of light, and we need relativity to describe the physics of the system. If we take the flat geometry, the relativistic MHD equations

$$\partial_\mu(\rho u^\mu) = 0, \tag{12}$$

$$\partial_\mu T^{\mu\nu} = 0, \tag{13}$$

$$\partial_t \mathbf{B} = \nabla \times (\mathbf{v} \times \mathbf{B}), \tag{14}$$

$$\nabla \cdot \mathbf{B} = 0, \tag{15}$$

where u^μ is the fluid four velocity and $T^{\mu\nu}$ is the stress-energy tensor of the fluid and the electromagnetic field, reduce to

$$\frac{\partial \mathbf{Q}}{\partial t} + \frac{\partial \mathbf{F}}{\partial x^1} = 0, \tag{16}$$

where

$$\mathbf{Q} = (S_1, S_2, S_3, B_2, B_3), \tag{17}$$

$$\mathbf{F} = (T_{11}, T_{12}, T_{13}, -E_3, E_2), \tag{18}$$

$$T_{ij} = -(E_i E_j + B_i B_j) + \frac{\delta_{ij}}{2}(E^2 + B^2), \tag{19}$$

$$\mathbf{S} = \mathbf{E} \times \mathbf{B}, \tag{20}$$

$$\mathbf{E} = -\frac{1}{B^2}\mathbf{S} \times \mathbf{B}. \tag{21}$$

Here, $\mathbf{E}$ is the electric field, $\mathbf{S}$ is the Poynting flux vector, and we use units such that the speed of light and π do not appear in the equations (see Komissarov, 2002). After solving equations along x^1 direction, we repeat similar procedures for x^2 and x^3 directions with appropriate rotation of indexes.

Scaling relations for relativistic Alfvénic MHD turbulence were first derived by Thompson and Blaes (1998) and were numerically tested by Cho (2005). Cho (2005) performed a numerical simulation of a decaying relativistic force-free[4] MHD turbulence with numerical resolution of 512^3 and calculated energy spectrum and anisotropy of eddy structures. At the beginning of the simulation, only Alfvén modes are present and the condition for critical balance, $\chi \equiv (bk_\perp)/(B_0 k_\parallel) \sim 1$, is satisfied (see Cho (2005, 2014) for heuristic discussions on the critical balance in relativistic force-free MHD turbulence). The left panel of Figure 3 shows energy spectrum of magnetic field at two different times. Although only large-scale (i.e. small k) Fourier modes are excited at t=0 (not shown), cascade of energy produces small-scale (i.e. large k) modes at later times. After $t \sim 3$, the energy spectrum decreases without changing its slope. The spectrum at this stage is very close to a Kolmogorov spectrum:

$$E(k) \propto k^{-5/3}. \tag{22}$$

Contours in the middle panel of Figure 3 shows shapes of eddies revealed by the second-order structure function for magnetic field. Note that the shape of eddies is measured in a local frame, which is aligned with the local mean magnetic field (see Cho et al, 2002b; Cho and Vishniac, 2000; Kowal and Lazarian, 2010, for details). The contour plot clearly shows existence of scale-dependent

[4] One can obtain the force-free condition from Maxwell's equations and the energy-momentum equation: $\partial_\mu T^{\nu\mu}_{(f)} = -F_{\nu\mu} J^\mu = 0$. Here, $F^{\nu\mu}$ is the electromagnetic field tensor.

anisotropy: smaller eddies are more elongated. The relation between the semi-major axis ($\sim l_\parallel \sim 1/k_\parallel$) and the semi-minor axis ($\sim l_\perp \sim 1/k_\perp$) of the contours fits very well the Goldreich-Sridhar type anisotropy:

$$k_\parallel \propto k_\perp^{2/3} \tag{23}$$

(see the right panel of Figure 3). All these results are consistent with the theoretical predictions in Thompson and Blaes (1998). A driven turbulence simulation in Cho (2014) also confirms the scaling relations.

Although the similarity between relativistic and non-relativistic Alfvénic turbulences may not be so surprising because the conditions for critical balance are identical, it has many astrophysical implications. So far, we do not fully understand turbulent processes in extremely relativistic environments, such as black hole/pulsar magnetospheres or gamma-ray bursts. The close similarities between extremely relativistic and non-relativistic Alfvénic turbulences enable us to understand the physical processes, e.g., reconnection, particle acceleration, etc., in such media better.

Due to the similarity, it is also possible that we can test non-relativistic theories using relativistic turbulence simulations. For example, Cho and Lazarian (2014) performed numerical simulations of imbalanced relativistic force-free MHD turbulence. The results of a simulation for 512^3 resolution is presented in Figure 4, in which the energy injection rate for Alfvén waves moving in one direction (dominant waves) is 4 times larger than that for waves moving in the other direction (sub-dominant waves). The left panel of Figure 4 shows that, even though the ratio of the energy injection rates is about $\sim$4, the ratio of the energy densities is about $\sim$100. The middle panel of the figure shows that the spectrum for the dominant waves is a bit steeper than a Kolmogorov spectrum, while that for the sub-dominant waves is a bit shallower. The right panel of the figure shows that the anisotropy of the dominant waves is a bit weaker than the Goldreich-Sridhar type anisotropy, while that of the sub-dominant waves is a bit stronger. All these results are consistent with the model of Beresnyak and Lazarian (2008) for non-relativistic Alfvénic MHD turbulence.

3.2 Fully relativistic MHD Turbulence

Fully relativistic MHD turbulence has been studied since 2009 (Zhang et al (2009); Inoue et al (2011); Beckwith and Stone (2011); Zrake and MacFadyen (2012, 2013); Garrison and Nguyen (2015), see also Radice and Rezzolla (2013) for non-magnetized turbulence). The results in Zrake and MacFadyen (2012, 2013) for the mean lab-frame Lorentz factor of $\sim$1.67 and numerical resolutions of up to 2048^3 confirm that there exists an inertial sub-range of relativistic velocity fluctuations with a -5/3 spectral index. They also found

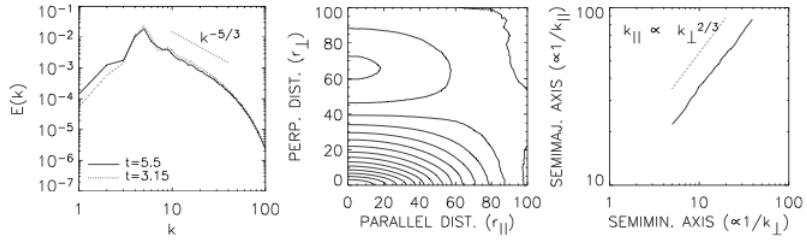

Fig. 3 Simulation of decaying relativistic force-free MHD turbulence. (Left) Energy spectrum is compatible with a Kolmogorov one. (Middle) Eddy shapes, represented by contours, show scale-dependent anisotropy: smaller eddies are more elongated. (Right) The anisotropy of eddy shape follows a Goldreich-Sridhar type anisotropy. Reproduced from Cho (2005) by permission of the AAS.

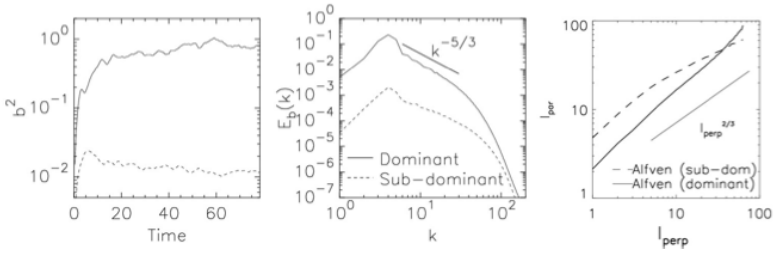

Fig. 4 Simulation of imbalanced relativistic force-free MHD turbulence. (Left) About a factor of 4 difference in energy injection rates results in a huge imbalance in energy densities. (Middle) The spectra for the dominant and the sub-dominant waves have different slopes: the dominant waves have a steeper spectrum. (Right) The degrees of anisotropy for the dominant and the sub-dominant waves are different: the dominant waves have a weaker anisotropy. Reproduced from Cho and Lazarian (2014) by permission of the AAS.

that intermittency based on the scaling exponents of the longitudinal velocity structure functions follows the She and Leveque (1994) model fairly well. On the other hand, simulations for unmagnetized relativistic turbulence with average Lorentz factors up to $\sim$1.7 revealed that relativistic effects enhance intermittency, so that the scaling exponents for high-order structure functions deviate from the prediction of the She-Leveque model significantly (Radice and Rezzolla, 2013).

We note that the decomposition of the relativistic MHD cascade into fundamental MHD modes has not been performed yet. The corresponding study in Cho and Lazarian (2002, 2003) and Kowal and Lazarian (2010) provided the framework for considering the separate Alfvénic, slow and fast mode cascades. We, however, expect that in analogy with what we already learned about the MHD turbulence, the results for relativistic and non-relativistic cases will not be much different.

4 Turbulent MHD reconnection

4.1 Sweet-Parker model and its generalization to turbulent media

The model of turbulent reconnection in LV99 generalizes the classical Sweet-Parker model (Parker, 1957; Sweet, 1958)[5]. In the latter model two regions with uniform *laminar* magnetic fields are separated by a thin current sheet. The speed of reconnection is given roughly by the resistivity divided by the sheet thickness, i.e.

$$V_{rec1} \approx \eta/\Delta. \tag{24}$$

For *steady state reconnection* the plasma in the current sheet must be ejected from the edge of the current sheet at the Alfvén speed, V_A. Thus the reconnection speed is

$$V_{rec2} \approx V_A \Delta/L_x, \tag{25}$$

where L_x is the length of the current sheet, which requires Δ to be large for a large reconnection speed. As a result, the overall reconnection speed is reduced from the Alfvén speed by the square root of the Lundquist number, $S \equiv L_x V_A/\eta$, i.e.

$$V_{rec,SP} = V_A S^{-1/2}. \tag{26}$$

The corresponding Sweet-Parker reconnection speed is negligible in astrophysical conditions as S may be 10^{16} or larger.

It is evident that the Sweet-Parker reconnection should be modified in the presence of turbulence. Figure 5 illustrates the modification that takes place. It is evident that the outflow in the turbulent flow is not limited by the microscopic region determined by resistivity, but is determined by magnetic field wandering. Therefore there is no disparity between L_x and Δ, e.g. for transAlfvénic turbulence they can be comparable. Actually, Figure 5 provides the concise illustration of the LV99 model of reconnection.

Adopting that the field wandering is the cause of the reconnection zone opening up, it is easy to calculate Δ in the regime when the turbulence injection scale L_i is less than L_x. Substituting $l_\parallel = L_i$ in Eq. (10) one finds that the perpendicular extend of the eddy at the injection scale is $L_i M_A^2$. The transverse contributions from different eddies at the injection scale are not correlated and therefore Δ is a result of random walk with a step of $L_i M_A^2$. The number of the steps along L_x is L_x/L_i and thus

$$\Delta \approx \left(\frac{L_x}{L_i}\right)^{1/2} L_i M_A^2, \quad L_i < L_x, \tag{27}$$

[5] The basic idea of the model was first discussed by Sweet and the corresponding paper by Parker refers to the model as "Sweet model".

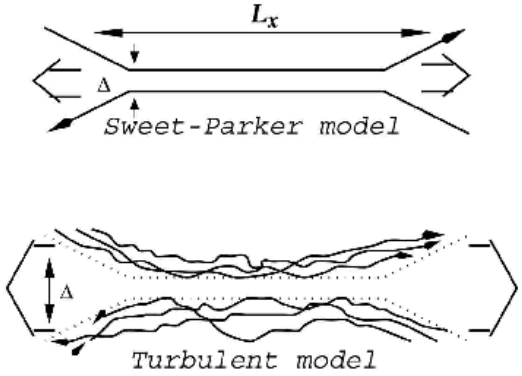

Fig. 5 *Upper plot*: Sweet-Parker model of reconnection. The outflow is limited to a thin width δ, which is determined by Ohmic diffusivity. The other scale is an astrophysical scale $L_x \gg \delta$. Magnetic field lines are laminar. Modified from Lazarian et al (2004). Reproduced by permission of the AAS.

and therefore

$$v_{rec,LV99} \approx V_A \left(\frac{L_i}{L_x}\right)^{1/2} M_A^2, \quad L_i < L_x, \tag{28}$$

which coincides with the LV99 result in this limit.

The result for $L_i > L_x$ can be obtained using the concept of Richardson dispersion following the approach in Eyink et al (2011). Richardson diffusion/dispersion can be illustrated with a simple hydrodynamic model. Consider the growth of the separation between two particles $dl(t)/dt \sim v(l)$, which for Kolmogorov turbulence is $\sim \alpha_t l^{1/3}$, where α_t is proportional to the energy cascading rate, i.e. $\alpha_t \approx V_L^3/L$ for turbulence injected with super-Alvénic velocity V_L at the scale L. The solution of this equation is

$$l(t) = [l_0^{2/3} + \alpha_t (t - t_0)]^{3/2}, \tag{29}$$

which at late times leads to Richardson dispersion or $l^2 \sim t^3$ compared with $l^2 \sim t$ for ordinary diffusion. This superdiffusive and even superballistic behavior, i.e. l^2 increases faster than t^2, can be easily understood if one takes into account that for points separated by the distance less than turbulence injection scale, the larger the separation of the points the larger the eddies that induce the point separation.

Both terms "diffusion and dispersion" can be used interchangeably, but keeping in mind that the Richardson process results in superdiffusion (see Lazarian and Yan, 2014, and references therein) we feel that it is advantageous to use the term "dispersion".

We again start with the Sweet-Parker reconnection. There magnetic field lines are subject to Ohmic diffusion. The latter induces the mean-square distance across the reconnection layer that a magnetic field-line can diffuse by resistivity in a time t given by

$$\langle y^2(t)\rangle \sim \lambda t. \tag{30}$$

where $\lambda = c^2/(4\pi\sigma)$ is the magnetic diffusivity. The field lines are advected out of the sides of the reconnection layer of length L_x at a velocity of order V_A. Therefore, the time that the lines can spend in the resistive layer is the Alfvén crossing time $t_A = L_x/V_A$. Thus, field lines that can reconnect are separated by a distance

$$\Delta = \sqrt{\langle y^2(t_A)\rangle} \sim \sqrt{\lambda t_A} = L_x/\sqrt{S}, \tag{31}$$

where S is Lundquist number. Combining Eqs. (25) and (31) one gets again the well-known Sweet-Parker result, $v_{rec} = V_A/\sqrt{S}$.

The difference with the turbulent case is that instead of Ohmic diffusion one should use the Richardson one (Eyink et al, 2011). In this case the mean squared separation of particles is $\langle|x_1(t) - x_2(t)|^2\rangle \approx \epsilon t^3$, where t is time, ϵ is the energy cascading rate and $\langle ...\rangle$ denote an ensemble averaging (see Kupiainen, 2003). For subAlfvénic turbulence $\epsilon \approx u_L^4/(V_A L_i)$ (see LV99) and therefore analogously to Eq. (31) one can write

$$\Delta \approx \sqrt{\epsilon t_A^3} \approx L_x (L_x/L_i)^{1/2} M_A^2, \tag{32}$$

where it is assumed that $L_x < L_i$. Combining Eqs. (25) and (32) one obtains

$$v_{rec,LV99} \approx V_A (L/L_i)^{1/2} M_A^2, \quad L_i > L_x, \tag{33}$$

that together with Eq. (28) provides the description of the reconnection for turbulent reconnection in the presence of sub-Alfvénic turbulence. Naturally, LV99 can be easily generalized for the case of superAlfvénic turbulence.

4.2 Temporal and spatial Richardson diffusion

We would like to stress that two formally different ways of obtaining LV99 reconnection rates have clear physical connection. In both cases we are dealing with magnetic field lines stochasticity, but the case of Richardson dispersion considers the evolution of magnetic fields lines in turbulent fluids, while magnetic field wandering presents the spatial distribution of magnetic field lines

for a given moment of time. In a sense the dispersion of magnetic field lines that was quantified in LV99[6] presents the Richardson dispersion in space.

While we employed the Alfvénic incompressible motions to describe the physics of Richardson dispersion, the process also takes place in compressible MHD turbulence. This is due to the fact, that Alfvénic cascade is a part and parcel of compressible MHD turbulence (Cho and Lazarian, 2003). We can, however, note parenthetically that even for turbulence of shocks, i.e. Burgers turbulence, the phenomenon of Richardson diffusion is present (Eyink et al, 2013).

4.3 Turbulent reconnection and violation of magnetic flux freezing

Magnetic flux freezing is a concept that is widely used in astrophysics. It is based on the Alfvén theorem, the proof of which is rather trivial for perfectly conductive laminar fluids. For laminar fluids of finite conductivity, the violation of Alfvén theorem becomes negligible as fluid conductivity increases. This, however, is not true for turbulent fluids. Turbulent reconnection as we discussed above induces reconnection diffusion. Mathematically the failure of the flux freezing is discussed in Lazarian et al (2015a). The numerical proof based on demonstrating of Richardson dispersion of magnetic field lines is in Eyink et al (2013).

4.4 Turbulent reconnection in compressible media

Two new effects become important in compressible media as compared to its incompressible counterpart that we discussed above. First of all, the density of plasmas changes in the reconnection region and therefore the mass conservation takes the form

$$\rho_{\rm i} v_{\rm rec,comp} L_x = \rho_{\rm s} V_A \Delta, \tag{34}$$

where $\rho_{\rm i}$ is the density of the incoming plasma far from the reconnection layer and $\rho_{\rm s}$ is the density of plasma in the reconnection layer.

In addition, the derivation of the magnetic field wandering rate that we discussed above was performed appealing to the Alfvénic component of MHD turbulence. Numerical simulations in Cho and Lazarian (2002, 2003) demon-

[6] The magnetic field wandering was discussed for an extended period to explain the diffusion of cosmic rays perpendicular to the mean magnetic field, but, as was shown in Lazarian and Yan (2014), those attempts employed scalings that were erroneous even for the hypothetical Kolmogorov turbulence of magnetic fields, for which they were developed.

strated that the Alfvénic component develops independently from the compressible MHD components in agreement with theoretical considerations in GS95. Therefore one can estimate the amplitude in incompressible Alfvénic perturbations by subtracting the contribution of the slow and fast modes from the total energy of the turbulent motions

$$u_L^2 \approx V_{total}^2 - V_{comp}^2. \tag{35}$$

Using both Eq. (34) and Eqs. (27) and (32) one can generalize the expression for the reconnection rate (compare to Eqs. (33), (28)):

$$v_{rec,comp} \approx V_A \frac{\rho_i}{\rho_s} \min\left[\left(\frac{L_i}{L_x}\right)^{1/2}, \left(\frac{L_x}{L_i}\right)^{1/2}\right] \frac{V_{total}^2 - V_{comp}^2}{V_A^2}. \tag{36}$$

If our turbulence driving is incompressible, another form of presenting the reconnection rate is useful if one takes into account the relation between the Alfvénic modes and the generated compressible modes obtained in Cho and Lazarian (2002)

$$\frac{V_{comp}^2}{V_{Alf}^2} \approx C_1 \frac{v_{inj}}{V_{Alf}}, \tag{37}$$

where C_1 is a coefficient which depends on the media equation of state. Taking into account the relation between the injection velocity and the resulting velocity in weak turbulence given by Eq. (37), one can rewrite Eq. (36) as

$$v_{rec,comp} \sim V_A \frac{\rho_i}{\rho_s} \min\left[\left(\frac{L_i}{L_x}\right)^{1/2}, \left(\frac{L_x}{L_i}\right)^{1/2}\right] \frac{v_{inj}^2(1 - C_1(v_{inj}/V_A))}{V_A^2}. \tag{38}$$

4.5 Turbulent reconnection in partially ionized gas

Partially ionized gas represents a complex medium where the ions co-exist with neutrals. Complex processes of ionization and recombination are taking place in turbulent partially ionized gas. However, in view of turbulent reconnection, the major feature of the partially ionized gas is that the turbulent motions in partially ionized gas are subject to damping which arises from both neutral-ion collisions and the viscosity associated with neutrals (see Lazarian et al, 2004; Xu et al, 2015, for a detailed discussion of the latter process). Figure 6 illustrates the damping of Alfvén modes in a typical environment of molecular cloud. The corresponding damping scales are substantially larger than those in the fully ionized gas, which poses the question of how turbulent reconnection is modified.

The reconnection in partially ionized gas was discussed on the basis of the Richardson dispersion in Lazarian et al (2015b). The essence of the ap-

proach is that on the scales at which Richardson dispersion is applicable, the magnetic fields are not frozen in and therefore magnetic reconnection is fast. Therefore the issue at which scale the reconnection is fast boils down to what is the scale of the onset of the Richardson dispersion description for the magnetic field lines.

It is natural to identify the magnetic field lines as subject to the Richardson dispersion as soon as the separation of the lines exceeds the size of the smallest turbulence eddy, i.e. the size of the critically damped eddy. In partially ionized gas the ion-neutral damping or viscosity determines this size. As the eddies are anisotropic, we would associate the damping scale with the parallel scale of the eddies $l_{\parallel,crit}$. Due to the shear induced by perpendicular motions associated with these eddies the magnetic field lines which are initially separated by r_{init} are spreading further and further from each other. The rate of line separating dr/dl is proportional to the $r/l_{\perp,crit}$ and this provides an exponential rate of separation. It is easy to show that separation becomes equal to $l_{\perp,crit}$ after the field lines are traced over a distance of

$$L_{RR} \approx l_{\parallel,crit} \ln(l_{\perp,crit}/r_{init}), \tag{39}$$

which was introduced by Rechester and Rosenbluth (1978) in the framework of "turbulence" with a single scale of driving. We follow Narayan and Medvedev (2003) and Lazarian (2006) associating this scale with the smallest turbulent eddies (cf. Chandran et al, 2000), as the smallest scales induce the largest shear. For r_{init} it is natural to associate this length with the separation of the field lines arising from the action of Ohmic resistivity on the scale of the critically damped eddies

$$r_{init}^2 = \eta l_{\parallel,crit}/V_A, \tag{40}$$

where η is the Ohmic resistivity coefficient. Taking into account Eq. (40) and that

$$l_{\perp,crit}^2 = \nu l_{\parallel,crit}/V_A, \tag{41}$$

where ν is the viscosity coefficient, one can rewrite Eq. (39) as:

$$L_{RR} \approx l_{\parallel,crit} \ln Pt, \tag{42}$$

where $Pt = \nu/\eta$ is the Prandtl number. This means that when the current sheets are much longer than L_{RR}, magnetic field lines undergo Richardson dispersion and according to Eyink et al (2011) the reconnection follows the laws established in LV99. At the same time on scales less than L_{RR} magnetic reconnection may be slow[7].

Additional effects, e.g. diffusion of neutrals perpendicular to magnetic field might potentially influence the reconnection rate (see Vishniac and Lazarian,

[7] Incidentally, this can explain the formation of density fluctuations on scales of thousands of AU, that are observed in the ISM.

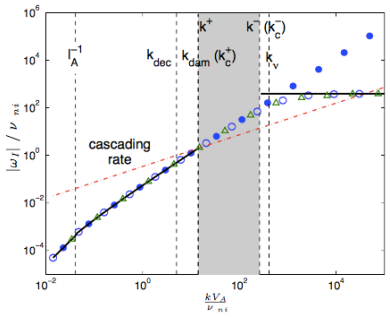

Fig. 6 Damping of Alfvénic turbulence in low beta partially ionized gas. The damping of turbulence happens when the rate of damping (solid line) intersects the dashed line corresponding to the cascading rate. From Xu et al (2015).

1999). Indeed, ions can recombine in the reconnection zone and this can allow the matter to outflow as a flow of neutrals. This outflow is not directly constrained by magnetic field and therefore Vishniac and Lazarian (1999) obtained large reconnection rates even for laminar magnetic fields provided that magnetic fields are perfectly anti-parallel and astrophysical medium is pure ionized hydrogen (see also a numerical study by Heitsch and Zweibel (2003)). The reconnection rates plummet in the presence of the guide field and heavy ions ("metals") which are subject to ionization by the ambient field. Therefore the effect of "ambipolar reconnection" is of marginal importance for most of the settings involving realistically turbulent media(see Lazarian et al, 2004).

5 Testing turbulent reconnection

Figure 7 illustrates results of numerical simulations of turbulent reconnection with turbulence driven using wavelets in Kowal et al (2009) and in real space in Kowal et al (2012).

As we show below, simulations in Kowal et al (2009, 2012) confirmed LV99 prediction that turbulent reconnection is fast, i.e. it does not depend on resistivity, and provided a good correspondence with the LV99 prediction on the injection power.

In the simulations subAlfvénic turbulence was induced, i.e. with the energy of kinetic motions less than the energy of magnetic field. Indeed, according to Eq. (28) $v_{rec,LV99} \sim u_l^2$. At the same time for the weak turbulence the injected power

$$P_{inj} \sim v_{inj}^2/\Delta t_{inj} \tag{43}$$

is equal to the cascading power given by Eq. (6). This provides a relation

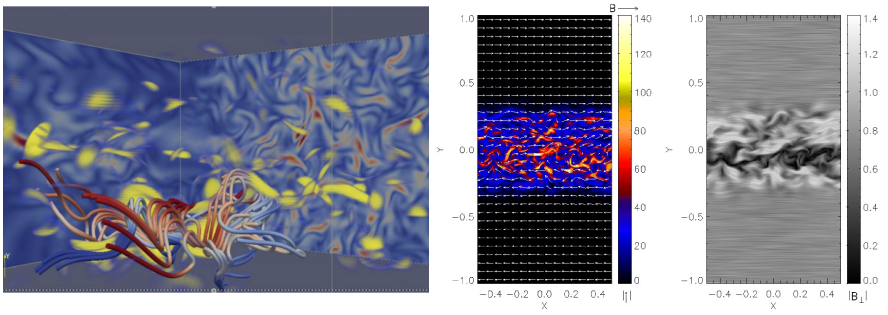

Fig. 7 Visualization of reconnection simulations in Kowal et al (2009, 2012). *Left panel*: Magnetic field in the reconnection region. *Central panel*: Current intensity and magnetic field configuration during stochastic reconnection. The guide field is perpendicular to the page. The intensity and direction of the magnetic field is represented by the length and direction of the arrows. The color bar gives the intensity of the current. *Right panel*: Representation of the magnetic field in the reconnection zone with textures. Reproduced from Kowal et al (2009) by permission of the AAS.

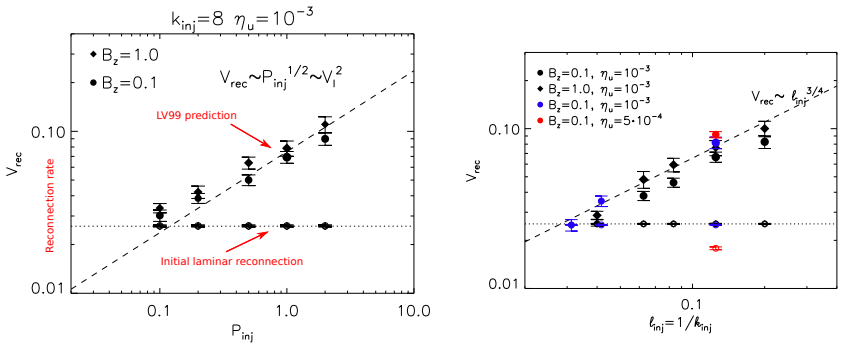

Fig. 8 *Left Panel* The dependence of the reconnection velocity on the injection power for different simulations with different drivings. The predicted LV99 dependence is also shown. P_{inj} and k_{inj} are the injection power and scale, respectively, B_z is the guide field strength, and η_u is the value of uniform resistivity coefficient. *Right Panel* The dependence of the reconnection velocity on the injection scale. Reproduced from Kowal et al (2012).

$$v_{rec,LV99} \sim u_l^2 \sim v_{inj} \sim P_{inj}^{1/2}. \tag{44}$$

The corresponding dependence is shown in Figure 8, left panel.

We also see some differences from the idealized theoretical predictions. For instance, the injection of energy in LV99 is assumed to happen at a given scale and the inverse cascade is not considered in the theory. Therefore, it is not unexpected that the measured dependence on the turbulence scale differs from the predictions. In fact, it is a bit more shallow compared to the LV99 predictions (see Figure 8, right panel).

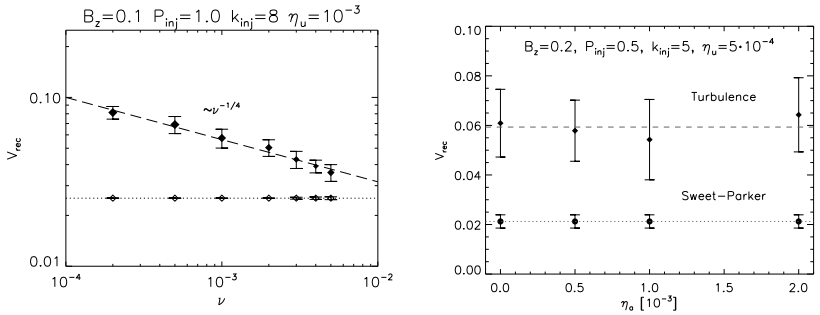

Fig. 9 *Left panel.* The dependence of the reconnection velocity on uniform viscosity in the 3D isothermal models of Sweet-Parker reconnection (open symbols) and reconnection enhanced by the presence of turbulence (closed symbols) from Kowal et al (2012). *Right panel.* The reconnection rate in models with anomalous resistivity for Sweet-Parker case (filled circles) and in the presence of turbulence (filled diamonds). We observe no dependence of the reconnection rate on the strength of anomalous effects. Reproduced from Kowal et al (2009).

The left panel of Figure 9 shows the dependence of the reconnection rate on explicit uniform viscosity obtained from the isothermal simulations of the magnetic reconnection in the presence of turbulence (Kowal et al, 2012). The open symbols show the reconnection rate for the laminar case when there was no turbulence driving, while closed symbols correspond to the mean values of reconnection rate in the presence of saturated turbulence. All parameters in those models were kept the same, except the uniform viscosity which varied from 10^{-4} to 10^{-2} in the code units. We believe that the dependence can be explained as the effect of the finite inertial range of turbulence than the effect of energy balance affected by viscosity or boundary conditions. For an extended range of motions, LV99 does not predict any viscosity dependence, if the dissipation scale lies much below the scale of current sheet. However, for numerical simulations the range of turbulent motions is very limited and any additional viscosity decreases the resulting velocity dispersion and the field wandering thus affecting the reconnection rate.

LV99 predicted that in the presence of sufficiently strong turbulence, plasma effects should not play a role. The accepted way to simulate plasma effects within MHD code is to use anomalous resistivity. The results of the corresponding simulations are shown in the right panel of Figure 9 and they confirm that the change of the anomalous resistivity does not change the reconnection rate.

As we discussed in section 3, the LV99 expressions can be obtained by applying the concept of Richardson dispersion to a magnetized layer. Thus by testing the Richardson diffusion of magnetic field, one also provides tests for the theory of turbulent reconnection. A successful direct testing of the temporal Richardson dispersion of magnetic field lines was performed in Eyink

et al (2013). The study confirmed that magnetic fields are not frozen in highly conducting fluids, as this follows from the LV99 theory.

Within the derivation adopted in LV99 current sheet is broad with individual currents distributed widely within a three dimensional volume and the turbulence within the reconnection region is similar to the turbulence within a statistically homogeneous volume. Numerically, the structure of the reconnection region was analyzed by Vishniac et al (2012) based on the numerical work by Kowal et al (2009). The results support LV99 assumptions about reconnection region being broad, the magnetic shear is more o less coincident with the outflow zone, and the turbulence within it is broadly similar to turbulence in a homogeneous system.

Another prediction that follows from LV99 theory is that the turbulence required for the process of turbulent reconnection can be generated by the process of turbulent reconnection. In particular, a theory of reconnection flares in low β (highly magnetized) plasmas was discussed in Lazarian and Vishniac (2009), while the expressions presenting reconnection rates in high β plasmas are presented in Lazarian et al (2015b).

6 Towards theory of turbulent relativistic reconnection

Recently, it has been recognized that the relativistically magnetized plasma, so-called Poynting-dominated plasma, plays an important role for many high energy astrophysical phenomena with relativistic outflows, such as pulsar wind nebulae, relativistic jets, and gamma-ray bursts. Those phenomena are believed to have a strongly magnetized compact object with rapid spin which naturally explains collimated jets or magnetized winds. The energy stored in the magnetic field initially needs to be converted into kinetic and radiation energy to explain the observations. However, the usual collisional magnetic field dissipation fails to explain the necessary dissipation rate. Relativistic turbulent magnetic reconnection is considered to be one of the most probable mechanism for the magnetic dissipation, and we review our recent development of the relativistic version of turbulent reconnection theory reported in Takamoto et al (2015).

We have seen that the relativistic balanced MHD turbulence in terms of theory is a clone of the GS95 model. We noticed that the imbalanced Alfvénic turbulence simulations provide very similar results in relativistic and non-relativistic cases [8]. As properties of Alfvénic turbulence dominate the LV99 reconnection, one can expect that the LV99 theory can be reformulated in terms of relativistic physics. However, instead of reformulating LV99 in terms of relativistic variables, for the time being, we shall use the theory in its non-

[8] Thus we can expect that the theory of imbalanced relativistic MHD can be also very similar to Beresnyak and Lazarian (2008) model.

relativistic formulation and seek its correspondence with the simulations of the relativistic turbulent reconnection.

For instance, it is obvious that effects of compressibility are likely to be more important in relativistic reconnection compared to its non-relativistic counterpart. This is because in Poynting-flux-dominated plasmas the magnetic field can induce a relativistic velocity in current sheets but the Alfvén velocity is limited by the light velocity, which allows the induced turbulence to be trans-Alfvénic one. Therefore, we use our results from section 4.4, in particular Eq. (36).

The comparison between the theoretical expectations and numerical simulations was performed in Takamoto et al (2015). The simulation is calculated using the relativistic resistive MHD code developed in Takamoto and Inoue (2011). The initial current sheet is assumed to be the relativistic Harris current sheet with uniform temperature $k_BT/mc^2 = 1$ where k_B, T, m, c are the Boltzmann constant, temperature, rest mass, and light velocity, respectively. The relativistic ideal gas is assumed, $h = 1 + (p/\rho c^2)(\Gamma/(\Gamma - 1))$ with $\Gamma = 4/3$ where h, p, ρ are the specific enthalpy, gas pressure, rest mass density. Following Kowal et al (2009), we used the open boundary in the direction perpendicular to the current sheet and parallel to the magnetic field, which corresponds to x and z direction. The periodic boundary is used in y direction. The guide field is basically omitted other than the runs used for obtaining Figure 13. Turbulence is driven by injecting a randomly determined turbulent flow every fixed time step. The turbulent flow has a flat kinetic energy spectrum and a characteristic wavelength is distributed around sheet width scale. More detailed setup is provided in Takamoto et al (2015). To quantify the reconnection rate the approach based on measurements of the change of the absolute value of magnetic flux in Kowal et al (2009) was used. In the calculations, we investigated turbulent reconnection in plasmas with the magnetization parameter from 0.04 (matter dominated) to 5 (Poynting dominated). Note that we assume a relativistic temperature, so that the plasma is always relativistic.

Figure 10 illustrates the magnetic field structure and gas pressure profile obtained by the simulations in Takamoto et al (2015). The magnetization parameter is $\sigma = 5$ and there is no guide field. The lines describe the magnetic field, and the background plane shows the gas pressure profile in units of the upstream magnetic pressure. It indicates the turbulence induces reconnecting points around the central sheet region. It also shows the magnetic field is wandering similarly to the non-relativistic case, which is responsible for determining the size of exhaust region and reconnection rate in LV99 theory. Note that the injected turbulence is sub-Alfvénic velocity but it can cause the stochastic magnetic field lines even in the case of Poynting-dominated plasma whose Alfvén velocity is relativistic.

Figure 11 (left panel) illustrates that in the process of relativistic magnetic reconnection the density inside the sheet changes substantially as the injected turbulent energy increases comparing with the energy flux of the reconnec-

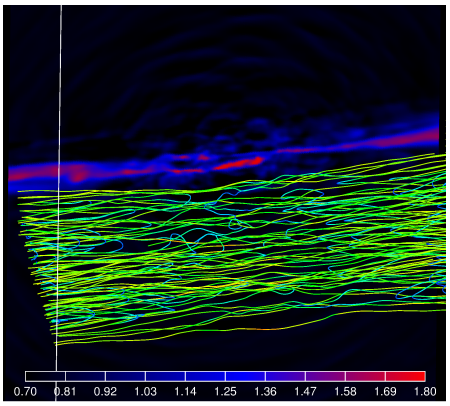

Fig. 10 Visualization of relativistic reconnection simulations in the case of the magnetization parameter $\sigma = 5$ from Takamoto et al (2015). The lines describe the magnetic field lines relating magnetic reconnection. The background plane shows the gas pressure profile in the unit of the upstream magnetic pressure. Similarly to the non-relativistic case, the magnetic field lines are wandering due to the injected turbulence, even in a Poynting-dominated plasma, which results in a wider reconnection exhaust region and large reconnection rate.

tion outflow. This is expected as can be seen from the simple arguments in Takamoto et al (2015). Indeed, the conservation of energy flux can be written as:

$$\rho_{\rm i} h_{\rm i} c^2 \gamma_{\rm i}^2 \left(1+\sigma_{\rm i}\right) v_{\rm i} L \ = \rho_{\rm s} h_{\rm s} c^2 \gamma_{\rm s}^2 \left(1+\sigma_{\rm s}\right) v_{\rm s} \delta, \tag{45}$$

where ρ, h, γ are the mass density, specific enthalpy, and Lorentz factor, respectively. c is the light velocity, and $\sigma \equiv B^2/4\pi\rho h c^2\gamma^2$ is the magnetization parameter. The subscript i, s means the variables defined in the inflow and outflow region, respectively. If we inject turbulence externally, this can be written as an input of turbulent energy into sheet, so that Equation (45) becomes

$$\begin{aligned}\rho_{\rm i} h_{\rm i} c^2 \gamma_{\rm i}^2 \left(1+\sigma_{\rm i}\right) v_{\rm i} L + (\rho_{\rm in} + B_0^2)\epsilon_{\rm inj} l_x l_z &= \rho_{\rm s} h_{\rm s} c^2 \gamma_{\rm s}^2 \left(1+\sigma_{\rm s}\right) v_{\rm s} \delta \\ &= \rho_{\rm s} h_{\rm s} c^2 \gamma_{\rm s}^2 \left(1+\sigma_{\rm s}\right) v_{\rm s} \sqrt{\epsilon t_A^3}, \end{aligned} \tag{46}$$

where ϵ is the energy injection rate of the turbulence, and we used $\mathbf{E}_{\rm turb}^2 = (\mathbf{v}_{\rm turb} \times \mathbf{B}_0)^2 \sim B_0^2 v_{\rm turb}^2/2$. l_x, l_z are the injection size along x and z axis. and Equation 32 is used in the second line. Note that the outflow energy flux is measured at the boundary of the reconnection outflow, and we assumed all the injected energy into the sheet is ejected as the outflow flux along the sheet, that is, the escaping components as compressible modes is assumed at least less than the Alfvénic component. Equation (46) shows that when the injected turbulence, ϵ, is small, the 2nd term in the left-hand side of the equation can be neglected, and the inflow velocity $v_{\rm i}$ increases as $\delta \propto \sqrt{\epsilon}$.

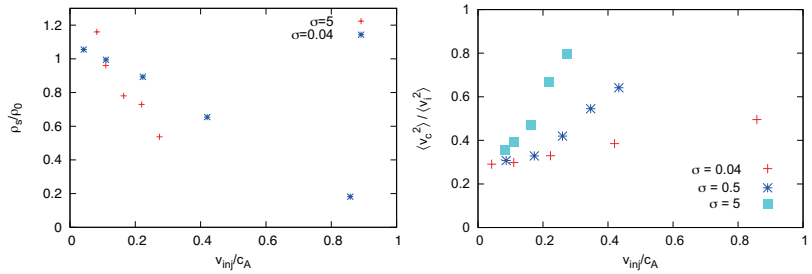

Fig. 11 *Left Panel* Variations of plasma density in relativistic reconnection. *Right Panel* Generation of compressible modes in relativistic reconnection. From Takamoto et al (2015).

However, if the injected turbulence is sufficiently strong, the neglected term increases as ϵ, and becomes comparable to the outflow flux which increases more slowly as $\epsilon^{1/2}$. In this case, combining with the conservation of mass,

$$\rho_{\rm i}\gamma_{\rm i}v_{\rm i}L = \rho_{\rm s}\gamma_{\rm s}v_{\rm s}\delta, \tag{47}$$

equation (46) gives

$$\frac{\rho_{\rm s}}{\rho_{\rm i}} = \frac{1}{(1+\sigma-\gamma_{\rm s})\gamma_{\rm s}}\left[2\sigma\gamma_{\rm s}^2 - (1+\sigma)\frac{\epsilon_{\rm inj}}{\sqrt{\epsilon t_A^3}}\frac{l_x l_z}{v_{\rm s}c^2}\right]. \tag{48}$$

This shows that the density ratio decreases as $\epsilon^{1/2} \propto v_{\rm inj}$, indicated as Figure 11 (left panel). The change of the matter density is an important factor in expression for the turbulent reconnection rate given by Eq. (36).

The other factor that we have to account is the decrease of the energy in Alfvénic turbulence as more energy is getting transferred to compressible modes for highly magnetized plasmas as illustrated by Figure 11 (right panel). Note, that the compressible component is obtained through the Helmholtz decomposition into solenoidal and compressible part rather than through the mode decomposition as in Cho and Lazarian (2002, 2003) or Kowal and Lazarian (2010). The latter procedure has not been adopted for the relativistic turbulence so far. Interestingly, the compressible component increases with the increase of the σ-parameter[9]. All in all, we conjecture that the compressible generalization of LV99 theory, see Eq. (38), can provide the description of relativistic reconnection.

Accounting for both effects Takamoto et al (2015) obtained a good correspondence between the theoretical predictions and numerical results. Figure 12 illustrates the dependence of reconnection rate on the strength of

[9] This may indicates a relation similar to one predicted by Galtier and Banerjee (2011), i.e. that the compressible component is proportional to B_0^2, exists even in relativistic MHD turbulence.

the injected turbulence with different magnetization cases. It shows that the maximal reconnection rate increases with the driving intensity (cf. Figure 8 (left panel)) in the sub-Alfvénic Mach number region. This can be basically explained by the law of turbulent reconnection given by LV99. However, as the injected Alfvén Mach number approaches to trans-Alfvénic region, the reconnection rate reaches a maximum value and even decreases with injected power. This is because the injected turbulence becomes compressible and the effect of compressibility should be accounted for (see §4.4). The detailed discussion including the compressiblity effects for relativistic reconnection is given in Takamoto et al (2015).

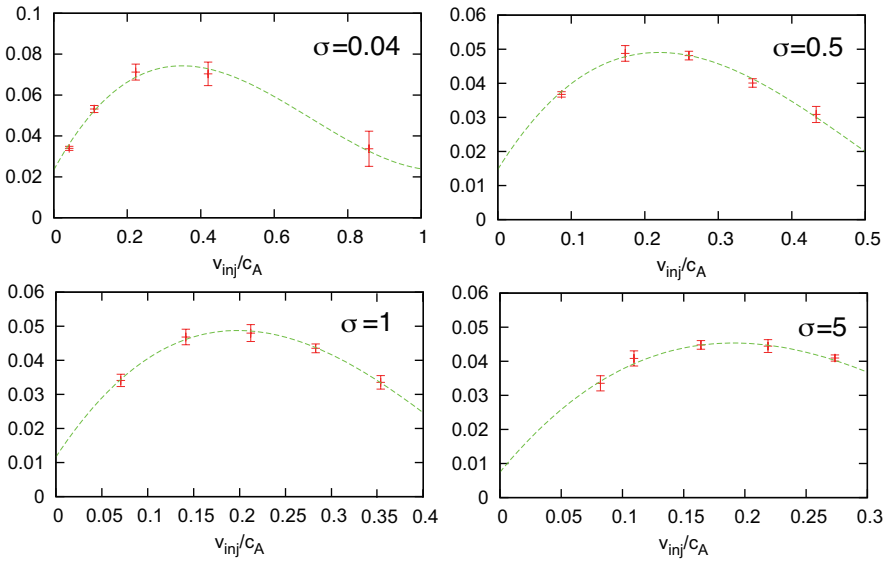

Fig. 12 Reconnection rate in terms of various magnetization parameters: $\sigma = 0.04, 0.5, 1, 5$. The green dashed curves are the modified turbulent reconnection law taking into account the effect of density decrease and compressible turbulence effects.

The guiding field effect is plotted in the left panel of Figure 13. Following Kowal et al (2009, 2012), we increased the guiding field while fixing the strength of reconnecting magnetic field component, that is, the total σ-parameter increases as increasing the guide field. The figure shows the reconnection rate that marginally depends of the guide field, which is very similar to the non-relativistic results obtained in Kowal et al (2009, 2012) presented in Figure 8. Thus we conclude that turbulent reconnection in relativistic and non-relativist cases is similar and a compressible generalization of the LV99 theory does reflect the main features of relativistic reconnection.

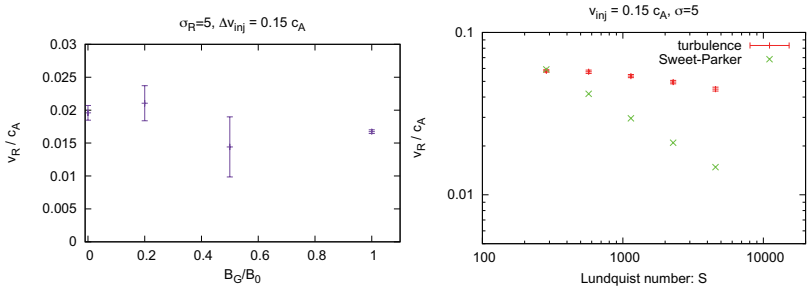

Fig. 13 *Left Panel.* Dependence of the reconnection rate on the guide field. *Right Panel.* Dependence of the reconnection rate on resistivity. From Takamoto et al (2015).

The right panel of Figure 13 shows that the reconnection rate does not show dependence on the resistivity. This supports the idea that the turbulent relativistic reconnection is fast.

The obtained results indicate that the reconnection rate can approach $0.3c$ if we assume a sufficient injection scale l, and this is enough to explain most cases of relativistic reconnection (see Lyutikov and Lazarian, 2013, for review). Note that that this result that satisfies the observational requirements is obtained with pure MHD rather than appealing to complicated collisionless physics, which manifests that fast relativistic reconnection is a robust process that takes place in various environments irrespectively on the the plasma collisionality.

Naturally, there are many important issues that must be studied in relation to turbulent relativistic reconnection and related processes. For instance, it is interesting and important to relate this reconnection with the relativistic analog of Richardson dispersion.

7 Reconnection with self-generated turbulence

Turbulence that drives turbulent reconnection is not necessarily pre-existent but can be generated as a result of reconnection. This was discussed in various publications starting with LV99 (see also Lazarian and Vishniac, 2009), but it is only with high resolution simulations that it became possible to observe this effect. Simulations by Lapenta (2008) that showed a transfer to fast reconnection in the MHD regime can be interpreted as spontaneous turbulent reconnection. The turbulence generation is seen in PIC simulations (see Karimabadi et al, 2014), incompressible simulations (Beresnyak, 2013) and compressible simulations (Oishi et al, 2015). The latter two papers identified the process of reconnection with fast turbulent reconnection. The shortcoming of these papers, however, is the use of periodic boundary conditions that do not allow studying steady state magnetic reconnection.

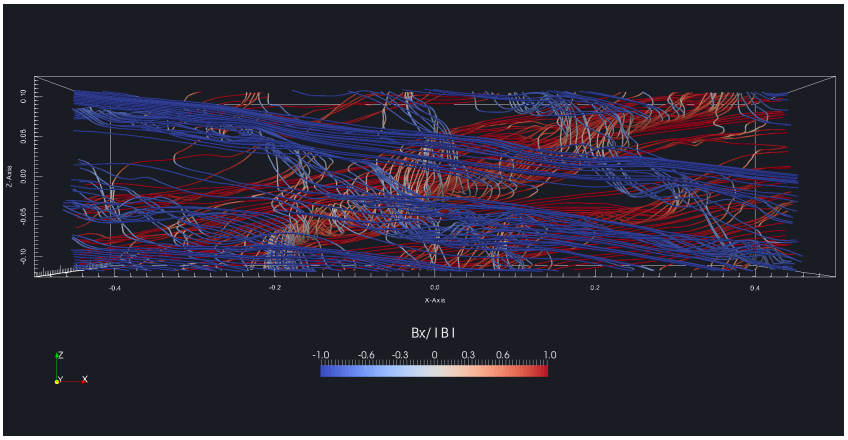

Fig. 14 Visualization of the magnetic field lines in the reconnection with self-generated turbulence as seen from the below of the current sheet plane. The colors correspond to the line orientation with respect to the X direction with red and blue being parallel and antiparallel to the X axis, respectively. We can recognize the organized field above and below the reconnection region and strongly turbulent flux tubes within the reconnection region. From Kowal et al (2015).

Below we present results from our calculations in Kowal et al (2015) where the open boundary conditions are adopted and the calculations are performed over several crossing times.

In the reconnection with a laminar configuration, the presence of initial noise in the velocity or magnetic fields results in the development of instabilities of the current sheet layer inducing its deformation and fragmentation. In such situations, we would expect that any deformation of the current sheet layer would grow, fed by the continuous plasma ejection from the local reconnection events ejecting more kinetic energy into the surrounding medium. In such a picture the injection scale would be related to the spatial separation of the randomly oriented small "jets" of the outflows from the local reconnection events. Those local outflows are estimated to have speeds comparable to the local Alfvénic speeds, i.e., capable of deforming local field. The corresponding bending of magnetic field lines is presented in Figure 14 in one of the models presented in Kowal et al (2015). The view from the bottom is shown, with the current sheet being perpendicular to the line of sight. In the initial configuration the magnetic field lines in the upper and bottom half of the domain are antiparallel with a small inclination due to the presence of the guide field. After some time, a turbulent region is developed around the midplane of the box due to the stochastic reconnection taking place there. This turbulent region is characterized by the magnetic line topology change. The lines are bent and twisted in this region, as seen in Figure 14. The color corresponds to the degree of line alignment with -1 (blue) being perfectly antiparallel and 1 (red) being perfectly parallel to the X direction.

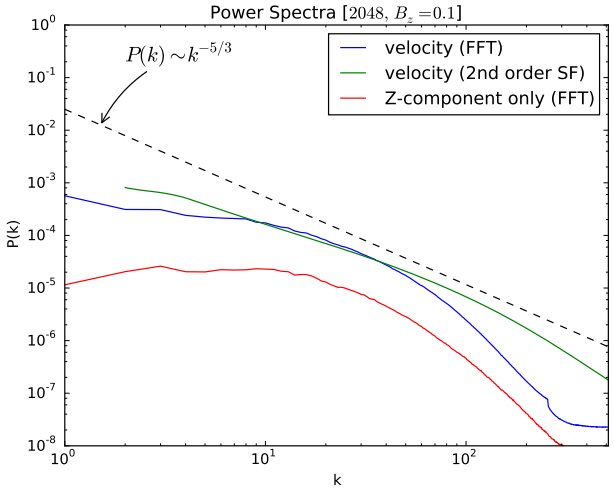

Fig. 15 Velocity power spectra obtained in a few different ways corresponding to the simulation snapshot shown in the previous figure. We show the power spectrum of the velocity obtained using the fast Fourier transform and the second order structure function (blue and green lines, respectively). The spectrum from the structure function approaches the Kolmogorov slope (dashed line) better, most probably because it is not sensitive to the type of boundary conditions. For comparison we show the power spectrum of Z-component (red line). From Kowal et al (2015).

In the next figure, Figure 15, we show the velocity power spectra calculated in two different ways for the snapshot shown in Figure 14. The blue line shows the classical power spectrum using the Fourier transform. However, since our domain is not periodic (periodicity is enforced only along the Z direction, otherwise the boundaries are open), the Fourier transform may not be a proper way to obtain the power spectra. Therefore, in the same figure we plot the velocity power spectrum obtained using the second-order structure function (SF) which is calculated in the real space and is insensitive to the type of the boundaries. Figure 15 shows that the power spectrum obtained from the structure function is more regular and approaches the Kolmogorov (dashed lines) slope better. This is a clear indication of the turbulence developed in such simulation.

For comparison, we also show the Fourier power spectrum of the Z-component of the velocity (red line in Fig. 15) for which should be less sensitive to the open boundaries since along this component we impose the periodicity. The power spectrum of this component is significantly weaker in amplitudes, especially in the large scale regime (small wave numbers k). This component is perpendicular both to the Y component, along which the new magnetic flux is brought, and to the X component, along which the reconnected flux is removed. In fast reconnection, both these components are comparable to the Alfvén speed. The weak amplitudes of the Z-component

of velocity may indicate strong anisotropies of the velocity eddies in the generated turbulence.

Some other features of the self-generated turbulence like the growth of the turbulence region were presented in Lazarian et al (2015c). For more detailed description of these models and analysis of the Kelvin-Helmholtz instability as the suspected mechanism of the injection, we refer to Kowal et al (2015).

8 Observational testing

The criterion for the application of LV99 theory is that the outflow region is much larger than the ion Larmor radius $\Delta \gg \rho_i$. This is definitely applicable for solar atmosphere, solar wind, but not for the magnetosphere. In the latter case the corresponding scales are comparable and plasma effects are important for reconnection.

8.1 Solar Reconnection

Solar reconnection was studied by Ciaravella and Raymond (2008) in order to test LV99 prediction of thick outflows. As we discussed earlier, the driving by magnetic reconnection is not isotropic and therefore the turbulence is strong from the injection scale. In this case

$$V_{rec} \approx U_{obs,turb}(L_{inj}/L_x)^{1/2}, \tag{49}$$

where $U_{obs,turb}$ is the spectroscopically measured turbulent velocity dispersion. Similarly, the thickness of the reconnection layer should be defined as

$$\Delta \approx L_x(U_{obs,turb}/V_A)(L_{inj}/L_x)^{1/2}. \tag{50}$$

The expressions given by Eqs. (49) and (50) can be compared with observations in Ciaravella and Raymond (2008). There, the widths of the reconnection regions were reported in the range from $0.08L_x$ up to $0.16L_x$ while the the observed Doppler velocities in the units of V_A were of the order of 0.1. It is easy to see that these values are in a good agreement with the predictions given by Eq. (50). The agreement obtained in the original comparison by Ciaravella and Raymond (2008) was based on the original expressions in LV99 that assume isotropic driving and weak turbulent cascading. Therefore the correspondence that the authors got was not so impressive and the authors concluded that both LV99 and Petschek X-point reconnection are potentially acceptable solutions.

At the same time, triggering of magnetic reconnection by turbulence generated in adjacent sites is a unique prediction of LV99 theory. This prediction

was successfully tested in Sych et al (2009), where the authors explained quasi-periodic pulsations in observed flaring energy releases at an active region above the sunspots as being triggered by the wave packets arising from the sunspots.

8.2 Solar Wind, Parker Spiral, Heliospheric Current Sheet

Solar wind reconnection was considered in Karimabadi and Lazarian (2013) review from the point of view of tearing plasma reconnection. The possibility of turbulent MHD reconnection was not considered in spite of the fact that $\Delta \gg \rho_i$, the deficiency of this review that was compensated in more recent review by Lazarian et al (2015b). There on the basis of studies of Solar wind in Lalescu et al (2015) it was concluded that the Solar wind reconnection is well compatible with LV99 theory (see Figure 16). The general features of the turbulent reconnection in MHD simulations correspond to the features of solar wind reconnection searched to identify reconnection events in the Solar wind (Gosling, 2007).

Similarly Eyink (2014) discussed some implications of turbulent reconnection for heliospheric reconnection, in particular for deviations from the Parker spiral model of interplanetary magnetic field. The latter model assumed frozen-in condition for magnetic field, which according to turbulent reconnection should be violated. Indeed, Burlaga et al (1982) studied the magnetic geometry and found "notable deviations" from the spiral model using Voyager 1 and 2 data at solar distances R=1-5 AU . The deviations from the theoretical expectations based on the frozen-in condition were substantiated by Khabarova and Obridko (2012), who presented evidence on the breakdown of the Parker spiral model for time- and space-averaged values of the magnetic field from several spacecraft (Helios 2, Pioneer Venus Orbiter, IMP8, Voyager 1) in the inner heliosphere at solar distances 0.3-5 AU. The latter authors interpret their observations as due to "a quasi-continuous magnetic reconnection, occurring both at the heliospheric current sheet and at local current sheets". Eyink (2014) estimated the magnetic field slippage velocities and related the deviation from Parker original predictions to LV99 reconnection. In addition, Eyink (2014) analyzed the data relevant to the region associated with the broadened heliospheric current sheet (HCS), noticed its turbulent nature and provided arguments on the applicability of LV99 magnetic reconnection model to HCS.

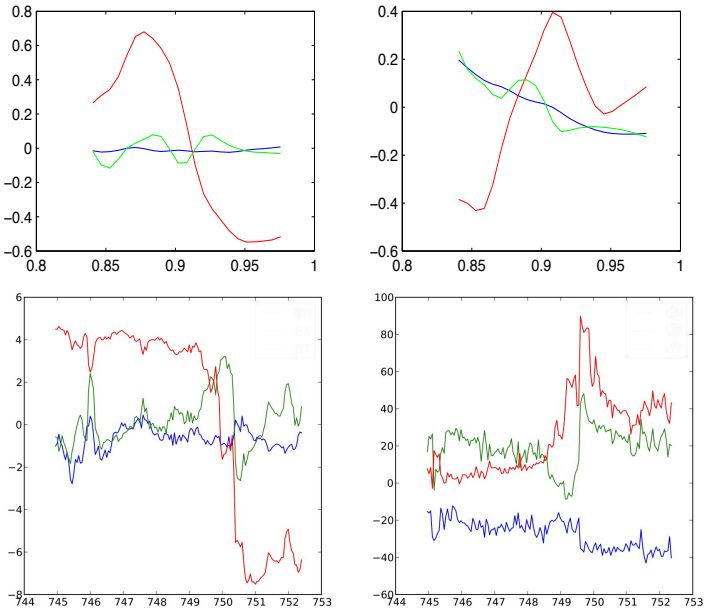

Fig. 16 Candidate Events for Turbulent Reconnection. *MHD Turbulence Simulation (Top Panels) and High-Speed Solar Wind (Bottom Panels).* The left panels show magnetic field components and the right panels velocity components, both rotated into a local minimum-variance frame of the magnetic field. The component of maximum variance in **red** is the apparent reconnecting component, the component of medium variance in green is the nominal guide-field direction, and the minimum-variance direction in blue is perpendicular to the reconnection layer. Reprinted figure with permission from Lalescu et al (2015). Copyright (2015) by the American Physical Society.

8.3 Indirect observational testing

Magnetic reconnection is extremely difficult to observe directly in generic astrophysical situations. Observations of the Sun, direct measurements of the Solar wind are notable exceptions. However, turbulent reconnection is happening everywhere in astrophysical turbulent magnetized environments and one can test the properties of reconnection by comparing the predictions that follow from the turbulent reconnection theory for particular astrophysical phenomena. This is an indirect way of testing turbulent reconnection and testing of different applications of the turbulent reconnection theory, including those that we cover in our review, also put turbulent reconnection at test.

We believe that the spectrum of turbulent fluctuations observed in astrophysical settings, e.g. in molecular clouds, galactic atomic hydrogen (see Lazarian, 2009, for review) testifies in favor of turbulent reconnection. Indeed, the measurements are consistent with numerical simulations (see Kowal

and Lazarian, 2010), which are performed in situations when turbulence induces fast reconnection. As it is discussed in Lazarian et al (2015b) it is the turbulent reconnection that makes the GS95 theory of strong turbulence self-consistent.

Similarly, we can say that testing of the processes of rapid diffusion of magnetic field in turbulent fluids that are mediated by turbulent reconnection, i.e. processes of reconnection diffusion that we discuss in §9.1, is also a testing of the underlying turbulent reconnection predictions. The same can be said about testing of the theories of gamma ray bursts, accretion disks, black hole sources that are based on the theory of turbulent reconnection (see examples of the comparison of theoretical predictions and observations in §9.3). We are sure that further detailed modeling of these phenomena based on the predictions of turbulent reconnection theory is an exciting avenue of research.

9 Implications of the theory

9.1 Reconnection diffusion: star formation and accretion disk evolution

Within the textbook theory of star formation, magnetic fields can influence and even control star formation at different stages, from the formation of the molecular cloud to the evolution of an accretion disk around a newly formed star (see Shu, 1983). The basic pillar of the corresponding theoretical constructions is that magnetic field is well frozen in highly conducting ionized component of the media so that the characteristic displacement of the magnetic field lines arising from Ohmic effects $\sqrt{\eta t}$ is much less than the scale of the system for any characteristic times of the system existence. This, however, assumes slow reconnection. But, because the media is typically only partially ionized, the segregation of matter and magnetic field can still happen at higher rate which is controlled by the differential drift of ions and neutrals, i.e. by the process that is termed *ambipolar diffusion*.

On the basis of LV99 theory, Lazarian (2005) suggested that the diffusion of magnetic fields in turbulent systems will be fast and independent of resistivity (see also Lazarian and Vishniac, 2009). This resulted in the concept that was termed "reconnection diffusion" in analogy to the earlier concept of ambipolar diffusion. A detailed discussion of the reconnection diffusion concept and its relation to star formation is presented in Lazarian (2014).

A formal theoretical proof that magnetic fields are not frozen in turbulent fluids is presented in Lazarian et al (2015b), while the numerical proof of the violation of flux freezing in turbulent media is provided through confirming the Richardson dispersion in Eyink et al (2013). This also follows directly

from LV99 and this is what motivated the reconnection diffusion concept. The corresponding review dealing with the reconnection diffusion is in Lazarian (2014) and we refer the interested reader to this extended work. In what follows, we just briefly discuss the reconnection diffusion concept as well as its implications.

The process of reconnection diffusion can be illustrated by Figure (17, upper), where the reconnection of flux tubes belonging to two adjacent eddies is shown. It is evident that, as a result of magnetic reconnection, the matter is being exchanged between the flux tubes and that in the presence of the cascade of turbulent motion at different scales the concept of the flux tube has a transient character, as the flux tubes evolve constantly being reformed by the motion of eddies at different scales.

Naturally, the concept of reconnection diffusion is applicable beyond the star formation range of problems. Quantitatively it boils down to understanding that on the scales larger than the turbulent injection scale the transfer of matter and magnetic field in superAlfvénic turbulence is happening through the turbulent advection by the eddies at the injection scale and the corresponding diffusion coefficient coincides with that in hydrodynamics, i.e. $k_{rec.diff,super} \approx 1/3 u_L L$. At the same time, for subAlfvénic turbulence the transfer is enabled by the strong turbulence eddies of the l_{trans} size and therefore the diffusion is reduced by the third power of Alfvén Mach number, i.e. $k_{rec.diff,sub} \approx 1/3 u_L L (u_L/V_A)^3$ (Lazarian, 2006). Interestingly enough, the same law, i.e. the reconnection diffusion coefficient proportional to M_A^3, follows from the theory of weak turbulence induced by the motions at the scales larger than t_{trans} (Lazarian 2006, see also Eyink et al 2011, henceforth ELV11). On the scales smaller than the injection scale the transport of magnetic field and matter follows the Richardson dispersion and accelerates as the scale under study increases. A discussion of the reconnection diffusion from the point of view of plasma slippage (see Eyink, 2014) is presented in Lazarian et al (2015b).

We would like to clarify that when we are talking about the suppression of reconnection diffusion in subAlfvénic turbulence, this is the suppression at the *large scales*, comparable with and larger than the injection scale. The local mixing of magnetic field lines at the scales l less than the scales at which turbulence is transferred to the strong regime, i.e. at scales smaller than $l_{trans} = LM_A^2$ (see Eq. (9)), is still given by the product lv_l and the corresponding small scale reconnection diffusion is governed by the Richardson dispersion and exhibits superdiffusive behavior. It relative inefficiency of reconnection diffusion at scales larger than l_{trans} that that impedes reconnection diffusion for large scales $\gg l_{trans}$.

The first numerical work that explored the consequences of reconnection diffusion for star formation was performed by Santos-Lima et al (2010), where the reconnection diffusion was applied to idealized setting motivated by magnetized diffuse interstellar medium and molecular clouds. A later paper by Leão et al (2013) provided a numerical treatment of the reconnection diffu-

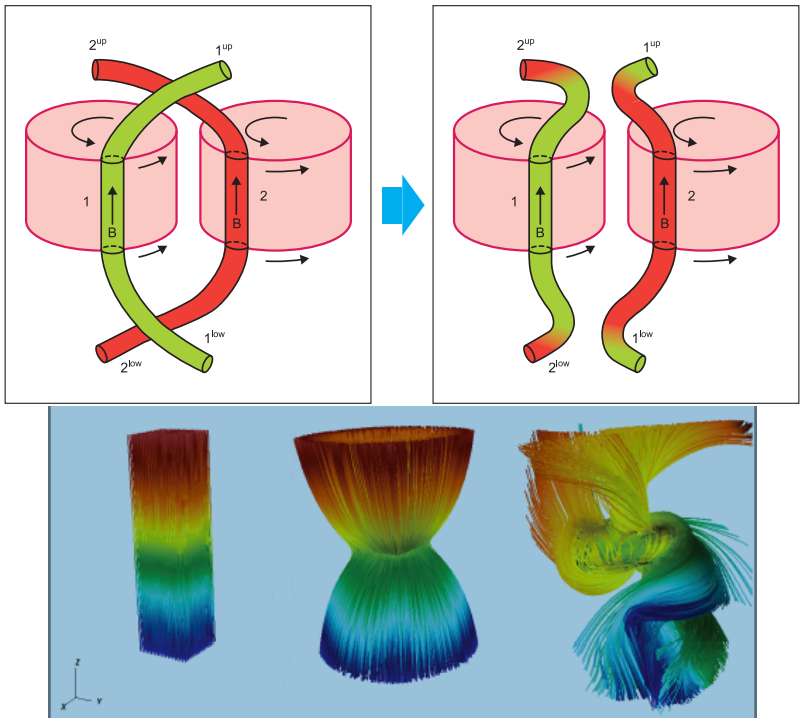

Fig. 17 Upper panel: Reconnection diffusion: exchange of flux with entrained matter. Illustration of the mixing of matter and magnetic fields due to reconnection as two flux tubes of different eddies interact. Only one scale of turbulent motions is shown. In real turbulent cascade such interactions proceed at every scale of turbulent motions. From Lazarian (2011). Lower panel: Visualization of magnetic field lines in a turbulent accretion disk. Illustration of the process using smoothed lines. From Casanova et al (2015).

sion for 3D collapse of self-gravitating clouds. In addition, the problem of the transport of angular momentum in protostellar accretion disks was considered in Santos-Lima et al (2012, 2013), where it was numerically demonstrated that the long-standing problem of magnetic breaking in the formation of protostellar accretion disks can be solved if disks are formed from turbulent media and therefore, reconnection diffusion takes place. A more recent study by Casanova et al (2015) (see Figure (17, lower) provides more evidence on the dominant role that reconnection diffusion plays in the disks.

It is important to understand that reconnection diffusion does not require magnetic fields changing their direction in space to the opposite one. In fact, in subAlfvénic turbulence, reconnection diffusion proceeds with magnetic field lines roughly directed along the mean magnetic field as shown in Figure 18, (left panel). When reconnection diffusion happens on the scales smaller than the turbulence injection scale, the spread of magnetic field lines obeys superdiffusive/superballistic Richardson dispersion law. In addition,

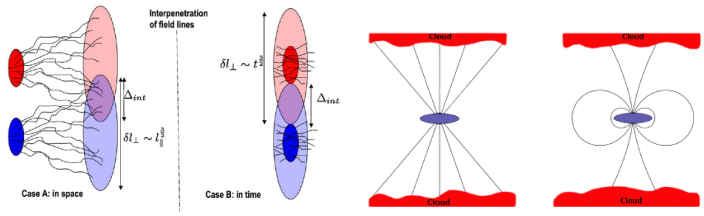

Fig. 18 *Left panel.* Case A. Microscopic physical picture of reconnection diffusion. Magnetized plasma from two regions is spread by turbulence and mixed up over the region Δ. Case B: description of the magnetic field line spreading with time. *Right Panel.* Change of the magnetic field configuration from the split monopole on the left to the dipole configuration on the right decreases the degree of coupling of the disk with the surrounding ISM without removing magnetic field from the disk. From Casanova et al (2015).

the process of reconnection diffusion that does not change the topology of magnetic flux in the statistical sense and the process of reconnection that radically changes the magnetic field topology can happen simultaneously, as it is illustrated in Figure 18 (right panel). There an additional process that facilitates the accretion disk formation is shown, namely, the change of magnetic field topology from the so-called "split monopole" to the dipole configuration. This change in turbulent interstellar plasmas is induced by turbulent reconnection and, similar to the reducing of the flux through the accretion disk that the reconnection diffusion entails, this topology change decreases the coupling of the accretion disk to the surrounding gas. Thus in reality both incarnations of turbulent reconnection process work together to solve the so-called "magnetic breaking catastrophe" problem.

A number of important implications of reconnection diffusion is discussed in Lazarian et al (2012). Those include the independence of the star formation rate on the metallicity in galaxies, star formation in galaxies with high ionization of matter, e.g. star formation in ultra-luminous infrared galaxies or ULIRGs (Papadopoulos et al, 2011), the absence of correlation between the magnetic field strength and gaseous density, etc.

These observational facts contradicting to the paradigm based on ambipolar diffusion naturally follow from the reconnection diffusion theory. Potential implications of reconnection diffusion in dynamos are also addressed in de Gouveia Dal Pino et al (2012).

Finally, we would like to compare the concept of reconnection diffusion with that of "turbulent ambipolar diffusion" (Fatuzzo and Adams, 2002; Zweibel, 2002). The latter concept is based on the idea that turbulence can create gradients of neutrals and those can accelerate the overall pace of ambipolar diffusion. The questions that naturally arise are (1) whether this process can proceed without magnetic reconnection and (2) what is the role of ambipolar diffusion in the process. Heitsch et al (2004) performed numerical simulations with 2D turbulent mixing of a layer with magnetic field

perpendicular to the layer and reported fast diffusion that was of the order of turbulent diffusivity number $V_L L$, *independent of ambipolar diffusion coefficient*. However, this sort of mixing can happen without reconnection only in a *degenerate case of 2D mixing* with exactly parallel magnetic field lines. In any realistic 3D case turbulence will bend magnetic field lines and the mixing process does inevitably involve reconnection. Therefore the 3D turbulent mixing in magnetized fluid must be treated from the point of view of reconnection theory. If reconnection is slow, the process in Heitsch et al (2004) cannot proceed due to the inability of magnetic field lines to freely cross each other (as opposed to the 2D case!). This should arrest the mixing and makes the conclusions obtained in the degenerate 2D case inapplicable to the 3D diffusion. If, however, reconnection is fast as predicted in LV99, then the mixing and turbulent diffusion will take place. However, such a diffusion is not expected to depend on the ambipolar diffusion processes, which is, incidentally, in agreement with results in Heitsch et al (2004), and will proceed at the the same rate in partially ionized gas as in fully ionize gas. The answers to the questions above are that turbulent diffusion in partially ionized gas is (1) impossible without fast turbulent reconnection and (2) independent of ambipolar diffusion physics. In this situation we believe that it may be misleading to talk about "turbulent ambipolar diffusion" in any astrophysical 3D setting.In fact, the actual diffusion in turbulent media is controlled by magnetic reconnection and is independent of ambipolar diffusion process!

9.2 Acceleration of energetic particles

Magnetic reconnection results in shrinking of magnetic loops and the charged particles entrained over magnetic loops get accelerated. This process was proposed by de Gouveia Dal Pino and Lazarian (2005, henceforth GL05) in the setting of LV99 reconnection.

The acceleration process is illustrated by Figure 19. Particles bounce back and forth between converging magnetic fluxes and undergo a first-order Fermi acceleration. An easy way to understand the process is by making an analogy with shock acceleration. As in shocks particles trapped within two converging magnetic flux tubes (moving to each other with the reconnection velocity V_R), will bounce back and forth undergoing head-on interactions with magnetic fluctuations and their energy after a round trip will increase by $< \Delta E/E > \sim V_R/c$, which implies a first-order Fermi process with an exponential energy growth after several round trips. Disregarding the particles backreaction one can get the spectrum of accelerated cosmic rays (GL05):

$$N(E)dE = const_1 E^{-5/2} dE. \quad (51)$$

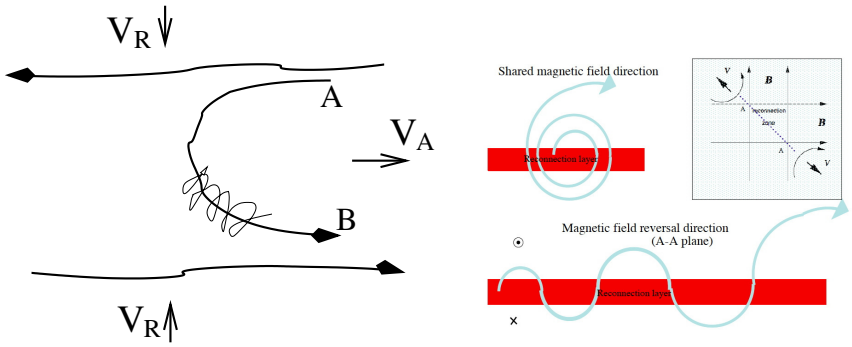

Fig. 19 *Left Panel:* Cosmic rays spiral about a reconnected magnetic field line and bounce back and forth at points A and B. The reconnected regions move towards each other with the reconnection velocity V_R. Reprinted figure with permission from Lazarian (2005). Copyright (2005), AIP Publishing LLC. *Right Panel:* Particles with a large Larmor radius gyrate about the guide/shared magnetic field. As the particle interacts with converging magnetized flow the particle gets energy gain during every gyration. Reprinted from Lazarian et al (2012).

This result of GL05 is valid for particle acceleration in the absence of compression (see Drury, 2012, for a study of the effects of compression which may result a flatter power-law spectrum).

Before the study in GL05, reconnection was discussed in the context of particle acceleration (e.g., Litvinenko, 1996; Shibata and Tanuma, 2001; Zenitani and Hoshino, 2001), but the first-order Fermi nature of the acceleration process was not revealed in these studies. A process similar to that in GL05 was later suggested as a driver of particle acceleration within collisionless reconnection in Drake et al (2006). The physics of the acceleration is the same, although GL05 appealed to 3D magnetic bundles (see, e.g., Figure 19), while Drake et al (2006) considered 2D shrinking islands. The latter is actually an artifact of the constrained 2D geometry. The difference in dimensions affects the acceleration efficiency as demonstrated numerically in Kowal et al (2011). Indeed, another way to view the first-order Fermi acceleration of particles entrained on the contracting helical magnetic loops in the embedded turbulence can be envisioned from the Liouville's theorem. In the process of loop contraction a regular increase of the particles energies takes place. The contraction of helical 3D loops is very different from the contraction of 2D islands. The most striking difference is that the latter stop contracting as the islands get circular in shape, while 3D loops shrink without experiencing such a constrain.

Several other studies explored particle acceleration in magnetic reconnection discontinuities considering collisionless plasmas (e.g. Drake et al, 2010; Jaroschek et al, 2004; Zenitani and Hoshino, 2008; Zenitani et al, 2009; Cerutti et al, 2013, 2014; Sironi and Spitkovsky, 2014; Werner et al, 2014; Guo et al, 2015), where magnetic islands or Petschek-like X-point configura-

tions of fast reconnection can be driven by kinetic instabilities (Shay et al, 2004; Yamada et al, 2010), or anomalous resistivity (e.g., Parker, 1979), see also Hoshino and Lyubarsky (2012) for a review. But as we discussed above, turbulence arises naturally in the process of reconnection which makes it necessary to consider turbulent reconnection for systems with sufficiently high Reynolds numbers.

Testing of particle acceleration in a large-scale current sheet with embedded turbulence to make reconnection fast was performed in Kowal et al (2012) and its results are presented in Figure 20. The simulations were performed considering 3D MHD domains of reconnection with the injection of 10,000 test particles. This study showed that the process of acceleration by large-scale turbulent reconnection can be adequately described by magnetohydrodynamics. Figure 20 depicts the evolution of the kinetic energy of the particles. After injection, a large fraction of test particles accelerates and the particle energy grows exponentially (see also the energy spectrum at $t = 5$ in the detail at the bottom right). This is explained by a combination of two effects: the presence of a large number of converging small scale current sheets and the broadening of the acceleration region due to the turbulence. The acceleration process is clearly a first-order Fermi process and involves large number of particles since the size of the acceleration zone and the number of scatterers naturally increases by the presence of turbulence. Moreover, the reconnection speed, which in this case is independent of resistivity (LV99, Kowal et al (2009)), determines the velocity at which the current sheets scatter particles that can be a substantial fraction of V_A. During this stage the acceleration rate is $\propto E^{-0.4}$ (Khiali et al, 2015a) and the particle power law index in the large energy tail is very flat (of the order of $1 - 2$).

The process of fast magnetic reconnection acceleration is expected to be widespread. In particular, it has been discussed in Lazarian and Opher (2009) as a cause of the anomalous cosmic rays observed by Voyagers and in Lazarian and Desiati (2010) as a source of the observed cosmic ray anisotropies.

Magnetic reconnection was also discussed in the context of acceleration of energetic particles in relativistic environments, like pulsars (e.g. Cerutti et al, 2013, 2014; Sironi and Spitkovsky, 2014; Uzdensky and Spitkovsky, 2014, see also Uzdensky this volume) and relativistic jets of active galactic nuclei (AGNs) (e.g. Giannios, 2010). The turbulent reconnection, that we argue in this review to be a natural process in astrophysical environments was considered for the environments around of black hole sources (GL05, de Gouveia Dal Pino et al, 2010b; Kadowaki et al, 2015; Singh et al, 2015; Khiali et al, 2015a; Khiali and de Gouveia Dal Pino, 2015); and gamma ray bursts (GRBs) (e.g. Zhang and Yan, 2011). The aforementioned studies are based on non-relativistic turbulent reconnection. However, the evidence that we provided above points out to a close similarity between the relativistic and non-relativistic turbulent reconnection. Thus we also expect that the process of particle acceleration in turbulent relativistic and non-relativistic reconnection to be similar. Naturally, this is an exciting topic for future re-

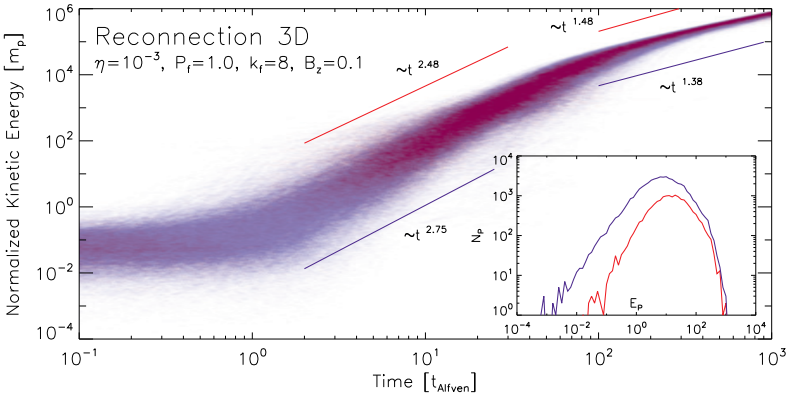

Fig. 20 Particle kinetic energy distributions for 10,000 protons injected in the fast magnetic reconnection domain. The colors indicate which velocity component is accelerated (red or blue for parallel or perpendicular, respectively). The energy is normalized by the rest proton mass. Subplot shows the particle energy distributions at $t = 5.0$. Models with $B_{0z} = 0.1$, $\eta = 10^{-3}$, and the resolution 256x512x256 is shown. Reprinted figure with permission from Kowal et al (2012). Copyright (2012) by the American Physical Society.

search. A more detailed discussion of the acceleration of energetic particles by turbulent reconnection can be found in de Gouveia Dal Pino et al (2014) and de Gouveia Dal Pino and Kowal (2015).

9.3 Flares of magnetic reconnection and associated processes

It is obvious that in magnetically dominated media the release of energy must result in the outflow that induces turbulence in astrophysical high Reynolds number plasmas. This inevitably increases the reconnection rate and therefore the energy release. As a result we get a *reconnection instability*. The details of such energy release and the transfer to turbulence have not been sufficiently studied yet. Nevertheless, on the basis of LV99 theory a simple quantitative model of flares was presented in Lazarian and Vishniac (2009), where it is assumed that since stochastic reconnection is expected to proceed unevenly, with large variations in the thickness of the current sheet, one can expect that some fraction of this energy will be deposited inhomogeneously, generating waves and adding energy to the local turbulent cascade. A more detailed discussion of the model is provided in Lazarian et al (2015b).

The applications of the theory range from solar flares to gamma ray bursts (GRBs). In particular, a model for GRBs based on LV99 reconnection was suggested in Lazarian et al (2003). It was elaborated and compared with observations in Zhang and Yan (2011), where collisions of magnetic turbulent

fluxes were considered. A different version of gamma ray bursts powered by turbulent reconnection proposed by Lazarian and Medvedev (2015) is based on kink instability. It is illustrated in Figure 21, left panel. Naturally, the model appeals to the relativistic turbulent reconnection that we described above. The difference of this model from other kink-driven models of GRBs (e.g. Drenkhahn and Spruit, 2002; Giannios and Spruit, 2006; Giannios, 2008; McKinney and Uzdensky, 2012) is that the kink instability also induces turbulence (Galsgaard and Nordlund, 1997; Gerrard and Hood, 2003) which drives magnetic fast reconnection as we discuss at length in this review. Within the GRB models in Zhang and Yan (2011) and Lazarian and Medvedev (2015) turbulent reconnection provides a good fit to the dynamics of GRBs.

In a similar line of research, Mizuno et al (2015), have performed 3D relativistic MHD simulations of rotating jets subject to the kink instability, considering several models with different initial conditions (i.e., different density ratios between the jet and the environment, different angular velocities, etc.) in order to explore fast magnetic reconnection, magnetic energy dissipation and a potential transition from magnetic to a matter dominated regime as predicted for GRBs and AGN jets (see also Rocha da Silva et al, 2015; McKinney and Uzdensky, 2012). The results indicate that a complex structure develops in the helical magnetic field due to the kink instability, developing several regions with large current densities, suggestive of intense turbulent reconnection (see Figure 21, right panel). Naturally, insufficient resolution limits the development of turbulence with a sufficiently extended inertial range. Therefore further numerical investigation of the process is required and, in fact, is in progress.

Turbulent reconnection is, unlike the Sweet Parker one, is a volume-filling reconnection. The magnetic energy is being released in the volume and is being transferred into the kinetic energy of fluid and energetic particles. Combined with fast rates of magnetic reconnection this makes the first-order Fermi process of particle acceleration efficient, which makes it plausible that a substantial part of the energy in magnetic field should be transferred to the accelerated particles. Therefore we believe that magnetic reconnection in the case of AGN jets (see Giannios (2010)) can be an copious source of high energy particles. In fact, numerical simulations of *in situ* particle acceleration by magnetic reconnection in the turbulent regions of relativistic jets (see de Gouveia Dal Pino and Kowal (2015)) demonstrate that the process can be competitive with the acceleration in shocks.

Particle acceleration arising from magnetic reconnection in the surrounds of black hole sources like active galactic nuclei (AGNs) and galactic black hole binaries (GHBs) has been also studied. In particular, GL05 (see also de Gouveia Dal Pino et al (2010b,a)) proposed that fast turbulent reconnection events occurring between the magnetic field lines arising from the inner accretion disk and the magnetosphere of the BH (see Figure 22) could be efficient enough to accelerate the particles and produce the observed core radio outbursts in GBHs and AGNs.

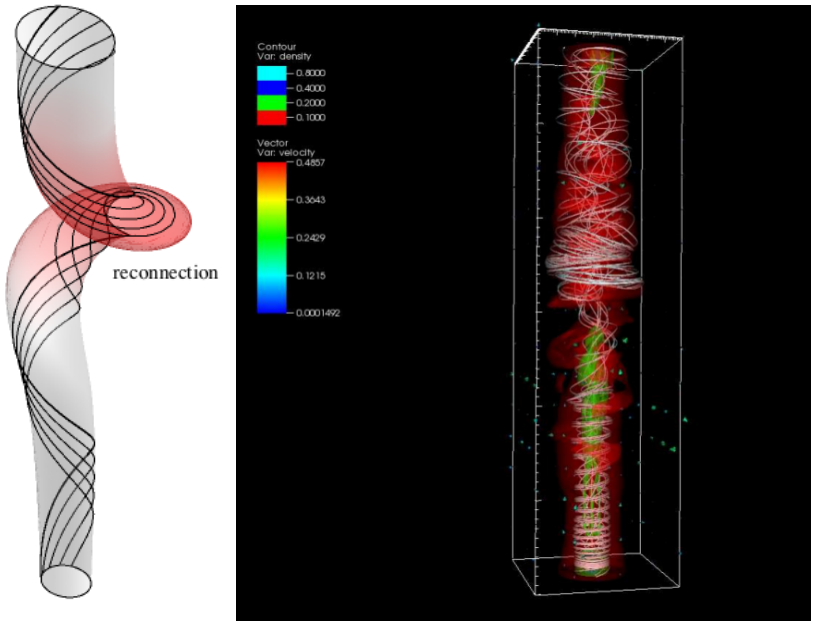

Fig. 21 *Left panel.* In the model by Lazarian and Medvedev (2015) magnetized jet with spiral magnetic field is being ejected. The spiral undergoes kink instability which results in turbulent reconnection. *Right panel* Numerical simulations of 3D relativistic jet that is subject to the kink instability and turbulent reconnection. From Mizuno et al (2015).

More recently, Kadowaki et al (2015) revisited the aforementioned model and extended the study to explore also the gamma-ray flare emission of these sources. The current detectors of high energy gamma-ray emission, particularly at TeVs (e.g., the FERMI-LAT satellite and the ground observatories HESS, VERITAS and MAGIC) have too poor resolution to determine whether this emission is produced in the core or along the jets of these sources. This study confirmed the earlier trend found in GL05 and de Gouveia Dal Pino et al (2010b) and verified that if fast reconnection is driven by turbulence, there is a correlation between the calculated fast magnetic reconnection power and the BH mass spanning 10^{10} orders of magnitude. This can explain not only the observed radio, but also the gamma-ray emission from GBHs and low luminous AGNs (LLAGNs). This match has been found for an extensive sample of more than 230 sources which include those of the so called *fundamental plane of black hole activity* (Merloni et al 2003) as shown in Figure 23. This figure also shows that the observed emission from blazars (i.e., high luminous AGNs whose jet points to the line of sight) and GRBs does not follow the same trend as that of the low luminous AGNs and GBHs, suggesting that the observed radio and gamma-ray emission in these cases is

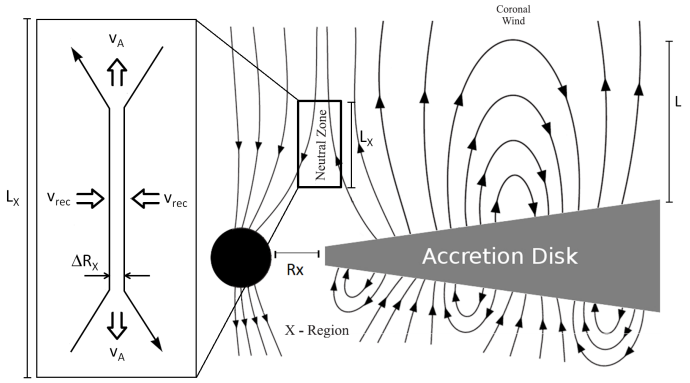

Fig. 22 Scheme of magnetic reconnection between the lines arising from the accretion disk and the lines of the BH magnetosphere. Reconnection is made fast by the presence of embedded turbulence in the reconnection zone (see text for more details). Particle acceleration occurs in the magnetic reconnection zone by a first-order Fermi process. Reprinted from Kadowaki et al (2015) by permission of the AAS.

not produced in the core of these sources. This result is actually exactly what one should expect because the jet in these systems points to the line of sight thus screening the nuclear emission, so that in these sources the emission is expected to be produced by another population of particles accelerated along the jet.

In another concomitant work, Singh et al (2015) explored the same mechanism, but instead of considering a standard thin, optically thick accretion disk as in the works above, adopted a magnetically-dominated advective accretion flow (M-ADAF; Narayan and Yi (1995); Meier (2012)) around the BH, which is suitable for sub-Eddington sources. The results obtained are very similar to those of Kadowaki et al (2015) depicted in Figure 23 ensuring that the details of the accretion physics are not relevant for the turbulent magnetic reconnection process which actually occurs in the corona around the BH and the disk.

The correlations found in Figure 23 (Kadowaki et al, 2015; Singh et al, 2015) have motivated further investigation. Employing the particle acceleration induced by turbulent reconnection and considering the relevant non-thermal loss processes of the accelerated particles (namely, Synchrotron, inverse Compton, proton-proton and proton-photon processes), Khiali et al (2015a) and Khiali et al (2015b) have computed the spectral energy distribution (SED) of several GBHs and LLAGNs and found that these match very well with the observations (see for instance Figure 24, which depicts the SED of the radio galaxy Cen A), especially at the gamma-ray tail, thus strengthening the conclusions above in favor of a core emission origin for the very high energy emission of these sources. The model also naturally explains

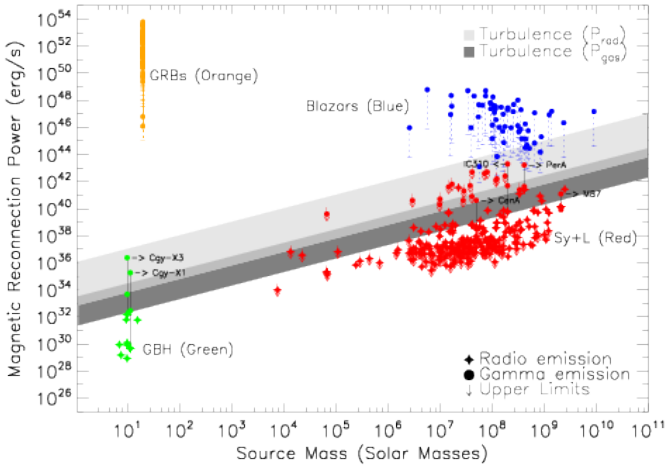

Fig. 23 Turbulent driven magnetic reconnection power against BH source mass (gray region) compared to the observed emission of low luminous AGNs (LLAGNs: LINERS and Seyferts), galactic black hole binaries (GBHs), high luminous AGNs (blazars) and gamma ray burst (GRBs). The core radio emission of the GBHs and LLAGNs is represented by red and green diamonds, the gamma-ray emission of these two classes is represented by red and green circles, respectively. In the few cases for which there is observed gamma-ray luminosity it is plotted the maximum and minimum values linking both circles with a vertical black line that extends down to the radio emission of each of these sources. The inverted arrows associated to some sources indicate upper limits in gamma-ray emission. For blazars and GRBs only the gamma-ray emission is depicted, represented in blue and orange circles, respectively. The vertical dashed lines correct the observed emission by Doppler boosting effects. The calculated reconnection power clearly matches the observed radio and gamma-ray emissions from LLAGNs and GBHs, but not that from blazars and GRBs. This result confirms early expectations that the emission in blazars and GRBs is produced along the jet and not in the core of the sources. Reprinted from Kadowaki et al (2015) by permission of the AAS.

the observed very fast variability of the emission. The same model has been also recently applied to explain the high energy neutrinos observed by the IceCube as due to LLAGNs (Khiali and de Gouveia Dal Pino, 2015).

10 Comparison of approaches to magnetic reconnection

10.1 Turbulent reconnection and numerical simulations

Whether MHD numerical simulations reflect the astrophysical reality depends on whether magnetic reconnection is correctly presented within these simulations. The problem is far from trivial. With the Lundquist number being

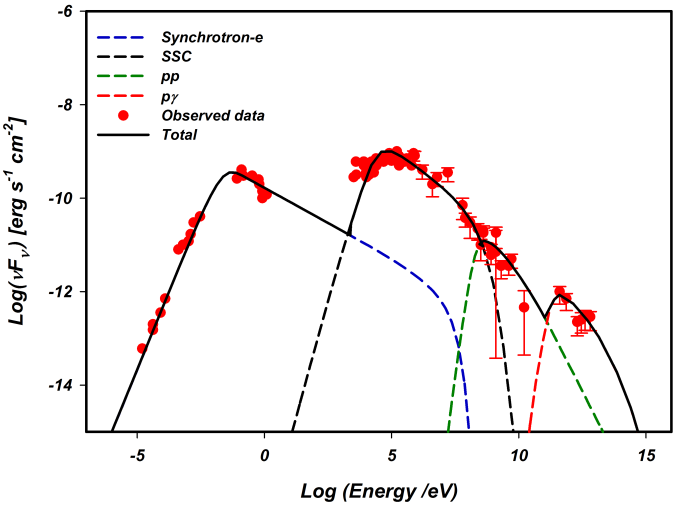

Fig. 24 Calculated spectral energy distribution (SED) for the AGN Cen A employing the turbulent magnetic reconnection acceleration model in the core region. The data depicted in the radio to optical energy range (10^{-5}eV $-$ 1eV) are from ISO and SCUBA and in the hard x-rays range from *Swift-BAT*, *OSSE* and *COMPTEL*. The data observed in the energies $10^8 - 10^{10}$eV are taken by *EGRET* and in the energies $10^8 - 10^{10}$eV by *Fermi-LAT*. The TeV data are taken by *HESS*. Reprinted from Khiali et al (2015b).

sometimes more than 10^{15} orders different, direct numerical simulation may potentially be very misleading. To deal with the issue Large Eddy Simulations (LES) approach may look promising (see Miesch et al, 2015). The catch here is that LES requires the explicit parametrization of reconnection rates. For instance, assume that following the ideas of tearing research we adopt a particular maximal value of reconnection speed, e.g. $0.01V_A$. This means that the motions where the fluids are moving with velocities larger than this chosen reconnection speed will be constrained. In MHD transAlfvénic turbulence, this would predict constraining the motions of eddies on the scales $[10^{-6}L, L]$ if we adopt the usual Kolmogorov $v \sim l^{1/3}$ scaling. This means that for this range of scales our results obtained with MHD turbulence theory are not applicable and the physics of many related processes is radically different. We believe that if wired this into LES, this will provide erroneous unphysical results.

From the point of view of the turbulent reconnection theory a normal MHD code reproduces magnetic reconnection correctly for turbulent regions, as for turbulent volumes the reconnection rate does not depend on resistivity and varies with the level of turbulence. As turbulence is the generic state of astrophysical fluids, the regions that are turbulent within numerical studies are correctly represented in terms of magnetic reconnection. On the contrary,

the regions where the turbulence is damped in simulations due to numerical diffusivity do not represent magnetic reconnection correctly. Situations where the initial set up is laminar requires following the development of turbulent reconnection and the prescriptions based on the corresponding simulation may be useful for parameterizing the process.

10.2 Turbulent reconnection versus tearing reconnection

It has been known for quite a while that Sweet-Parker current sheet is unstable to tearing and this can affect the reconnection rate (see Syrovatskii, 1981, LV99). What was a more recent development is that the 2D current sheet starting with a particular Lundquist number larger than 10^4 develops fast reconnection (see Loureiro et al, 2007; Uzdensky et al, 2010), i.e. reconnection that does not depend on the fluid resistivity. The study of tearing momentarily eclipsed the earlier mainstream research of the reconnection community, which attempted to explain fast reconnection appealing to the collisionless plasma effects that were invoked to stabilize the Petschek-type X point configuration for reconnection (Shay et al, 1998; Drake, 2001; Drake et al, 2006). We view this as a right step in abandoning the artificial extended X point configurations the stability of which in the situation of realistic astrophysical forcing was very doubtful (see discussion in LV99). However, we believe that tearing by itself does not provide a generic solution for the astrophysical reconnection.

To what extend tearing is important for the onset of 3D turbulent reconnection should be clarified by the future research. Here we can provide arguments suggesting that tearing inevitably transfers to turbulent reconnection for sufficiently large Lundquist numbers S. Indeed, from the mass conservation constraint requirement in order to have fast reconnection one has to increase the outflow region thickness in proportion to L_x, which means the proportionality to the Lundquist number S. The Reynolds number Re of the outflow is $V_A\Delta/\nu$, where ν is viscosity, grows also as S. The outflow gets turbulent for sufficiently large Re. It is natural to assume that once the shearing rate introduced by eddies is larger than the rate of the tearing instability growth, the instability should get suppressed.

If one assumes that tearing is the necessary requirement for fast reconnection, this entails the conclusion that tearing should proceed at the critically damped rate, which implies that the Re number and therefore Δ should not increase. This entails, however, the decrease of reconnection rate driven by tearing in proportion $L_x \sim S$ as a result of mass conservation. As a result, the reconnection should stop being fast. Fortunately, we know that turbulence itself provides fast reconnection irrespectively whether tearing is involved or not.

We also note that tearing reconnection in numerical simulations provides the reconnection rate around $0.01V_A$ for collisional and somewhat larger rates for collisionless reconnection. These limitations are incompatible with the requirements of astrophysical reconnection, which, for instance, requires reconnection of the order of V_A for large scale eddies in transAlfvénic turbulence. In addition, fixed reconnection rates do not explain why observed reconnection may sometimes be slow and sometimes fast.

10.3 Turbulent reconnection versus turbulent resistivity and mean field approach

Attempts to describe turbulent reconnection introducing some sort of turbulent resistivity are futile and misleading. It is possible to show that "turbulent/eddy resistivity" description has fatal problems of inaccuracy and unreliability, due to its poor physical foundations for turbulent flow. It is true that coarse-graining the MHD equations by eliminating modes at scales smaller than some length l will introduce a "turbulent electric field", i.e. an effective field acting on the large scales induced by motions of magnetized eddies at smaller scales. However, it is well-known in the fluid dynamics community that the resulting turbulent transport is not "down-gradient" and not well-represented by an enhanced diffusivity. Indeed, turbulence lacks the separation in scales to justify a simple "eddy-resistivity" description. As a consequence, energy is often not absorbed by the smaller eddies, but supplied by them, a phenomenon called "backscatter". The turbulent electric field often creates magnetic flux rather than destroys it.

If we know the reconnection rate, e.g. from LV99, then an eddy-resistivity can always be tuned by hand to achieve that rate. But this is not science. While the tuned reconnection rate will be correct by construction, other predictions will be wrong. The required large eddy-resistivity will smooth out all turbulence magnetic structure below the coarse-graining scale l. In reality, the turbulence will produce strong small-scale inhomogeneities, such as current sheets, from the scale l down to the micro-scale. In addition, field-lines in the flow smoothed by eddy-resistivity will not show the explosive, super-diffusive Richardson-type separation at scales below l. These are just examples of effects that will be lost if the wrong concept of "eddy resistivity" is adopted. Note, that the aforementioned are important for understanding particle transport/scattering/acceleration in the turbulent reconnection zone. We can also point out that in the case of relativistic reconnection that we also deal with in this review, turbulent resistivities will introduce non-causal, faster than light propagation effects. Nevertheless, the worst feature of the crude "eddy-resistivity" parametrization is its unreliability: because it has no scientific justification whatsoever, it cannot be applied with any confidence to astrophysical problems.

We would like to stress that the fast turbulent reconnection concept is definitely not equivalent to the dissipation of magnetic field by resistivity. While the parametrization of some particular effects of turbulent fluid may be achieved in models with different physics, e.g. of fluids with enormously enhanced resistivity, the difference in physics will inevitably result in other effects being wrongly represented by this effect. For instance, turbulence with fluid having resistivity corresponding to the value of "turbulent resistivity" must have magnetic field and fluid decoupled on most of its inertia range turbulent scale, i.e. the turbulence should not be affected by magnetic field in gross contradiction with theory, observations and numerical simulations. Magnetic helicity conservation which is essential for astrophysical dynamo should also be grossly violated[10].

The approach that we advocate is quite different. It is not based on coarse-graining. The stochasticity of magnetic field-lines is a real, verified physical phenomenon in turbulent fluids. Whereas "eddy-resistivity" ideas predict that magnetic flux is destroyed by turbulence, we argue that turbulent motions constantly change connectivity of magnetic field lines without dissipating magnetic fields. Being moved by fluid motions the stochastic world-lines in relativistic turbulence do remain within the light-cone and no non-causal effects such as produced by "eddy-resistivity" being entailed (see also ELV11).

Understanding that "resistivity arising from turbulence" is not a real plasma non-ideality "created" by the turbulence is essential for understanding why mean field approach fails in dealing with reconnection in turbulent fluids. Indeed, turbulence induced apparent non-ideality is dependent on the length and timescales of the averaging and it emerges only as a consequence of observing the plasma dynamics at a low resolution, so that the observed coarse-grained velocity and magnetic field do not satisfy the true microscopic equations of motion. It is obvious, that coarse-graining or averaging is a purely passive operation which does not change the actual plasma dynamics. The non-ideality in a turbulent plasma observed at length-scales in the inertial-range or larger is a valid representation of the effects of turbulent eddies at smaller scales. However, such apparent non-ideality cannot be represented by an effective "resistivity", a representation which in the fluid turbulence literature has been labeled the "gradient-transport fallacy" (Tennekes and Lumley, 1972).

A recent paper that attempts to address turbulent reconnection using mean field approach is Guo et al (2012), where ideas originally proposed in Kim and Diamond (2001) were modified and extended. Thus while the study in Kim and Diamond (2001) concluded that turbulence cannot accelerate reconnection, the more recent study came to the opposite conclusions. The expressions for reconnection rates in Guo et al (2012) are different from those

[10] Increasing the resistivity to the values required to account for the diffusivities that arise from turbulent reconnection would make astrophysical dynamos resistive or slow, in gross contradiction to the fact that astrophysical dynamos operate in fluids with engligible resistivity and therefore can be only modeled by "fast dynamo" (see Parker 1979).

in LV99 and grossly contradict the results of numerical testing of turbulent reconnection in Kowal et al (2009). Another model of turbulent reconnection based on the mean field approach is presented in Higashimori and Hoshino (2012).

The mean field approach invoked in the aforementioned studies is plagued by poor foundations and conceptual inconsistencies (ELV11). In such an approach effects of turbulence are described using parameters such as anisotropic turbulent magnetic diffusivity experienced by the fields once averaged over ensembles. The problem is that it is the lines of the full magnetic field that must be rapidly reconnected, not just the lines of the mean field. ELV11 stress that the former implies the latter, but not conversely. No mean-field approach can claim to have explained the observed rapid pace of magnetic reconnection unless it is shown that the reconnection rates obtained in the theory are strictly independent of the length and timescales of the averaging.

Other attempts to get fast magnetic reconnection from turbulence are related to the so-called hyper-resistivity concept (Strauss, 1986; Bhattacharjee and Hameiri, 1986; Hameiri and Bhattacharjee, 1987; Diamond and Malkov, 2003), which is another attempt to derive fast reconnection from turbulence within the context of mean-field resistive MHD. Apart from the generic problems of using the mean field approach, the derivation of the hyper-resistivity is questionable from yet another point of view. The form of the parallel electric field is derived from magnetic helicity conservation. Integrating by parts one obtains a term which looks like an effective resistivity proportional to the magnetic helicity current. There are several assumptions implicit in this derivation, however. Fundamental to the hyper-resistive approach is the assumption that the magnetic helicity of mean fields and of small scale, statistically stationary turbulent fields are separately conserved, up to tiny resistivity effects. However, this ignores magnetic helicity fluxes through open boundaries, essential for stationary reconnection, that vitiate the conservation constraint (see more discussion in LV99, ELV11 and Lazarian et al, 2015b).

10.4 Turbulent reconnection: 3D versus 2D

A lot of physical phenomena are different in 3D and 2D with hydrodynamic turbulence being a striking example. However, due to numerical constraints many numerical studies of the physical phenomena are initially attempted in the systems of reduced dimensions. Whether the physics in the system of reduced dimensions is representative of the physics of the 3D system in such situations must be theoretically justified and tested. For magnetic reconnection the justification of similarity of systems of reduced dimention is difficult, as crucial differences between 2D and 3D magnetic reconnection are stressed e.g. in Priest (this volume) and also in publications by Boozer (2012, 2013).

There it is shown that an extrapolation from reconnection physics obtained in 2D to 3D is poorly justified. In what follows, we add additional points why we do not believe that 2D turbulent reconnection can be a guide for our understanding of the 3D astrophysical reconnection.

Matthaeus and Lamkin (1985, 1986) explored numerically turbulent reconnection in 2D. As a theoretical motivation the authors emphasized analogies between the magnetic reconnection layer at high Lundquist numbers and homogeneous MHD turbulence. They also pointed out various turbulence mechanisms that would enhance reconnection rates, including multiple X-points as reconnection sites, compressibility effects, motional electromotive force (EMF) of magnetic bubbles advecting out of the reconnection zone. However, the authors did not realize the importance of stochastic magnetic field wandering and they did not arrive at an analytical prediction for the reconnection speed. Although an enhancement of the reconnection rate was reported in their numerical study, but the setup precluded the calculation of a long-term average reconnection rate.

We would like to stress the importance of this study in terms of attracting the attention of the community to the influence of turbulence on reconnection. However, the relation of this study with LV99 is not clear, as the nature of turbulence in 2D is different. In particular, shear-Alfvén waves that play the dominant role in 3D MHD turbulence according to GS95 are entirely lacking in 2D, where only pseudo-Alfvén wave modes exist.

We believe that the question whether turbulent reconnection is fast in 2D has not been resolved yet if we judge from the available publications. For instance, in a more recent study along the lines of the approach in Matthaeus and Lamkin (1985), i.e. in Watson et al (2007), the effects of small-scale turbulence on 2D reconnection were studied and no significant effects of turbulence on reconnection was reported. Servidio et al (2010) have more recently made a study of Ohmic electric fields at X-points in homogeneous, decaying 2D MHD turbulence. However, they studied a case of small-scale magnetic reconnection and their results are not directly relevant to the issue of reconnection of large-scale flux tubes that we deal with in this review. The study by Loureiro et al (2009) and that by Kulpa-Dybeł et al (2010) came to different conclusions on whether 2D turbulent reconnection is fast in 2D. Irrespectively of the solution of this particular controversy, we believe that 2D turbulent reconnection is radically different from that in 3D, as both the nature of MHD turbulence that drives the reconnection and the nature of 2D and 3D reconnection processes are very different (see our discussions above).

10.5 Turbulent reconnection and small scale reconnection events

Magnetic reconnection is frequently presented as a particular example of a problem where the resolving processes from the smallest to the largest scales is vital. We argue that this is not the case of turbulent reconnection. Indeed, turbulence is a phenomenon in which the dynamics of large eddies is not affected by the microphysics of the dissipation at small scales. Similarly, it was shown in LV99 that the rate of turbulent reconnection does not depend on the rate of local reconnection events. As a result, the rate of turbulent reconnection is expected to be the same in collisionless and collisional media. Therefore the arguments that tearing decreases the length of reconnection layers transferring reconnection in collisionless regime and this way makes the reconnection faster are not applicable to turbulent reconnection.

We also stress that the small scale plasma turbulence that can change the local resistivity and local reconnection rates (see Karimabadi & Lazarian 2014 for a review) does not affect the global rate of turbulent reconnection. The latter is a MHD phenomenon that depends on the properties of turbulence only.

11 Final remarks

11.1 Suggestive evidence

There are pieces of evidence that are consistent with turbulent reconnection and can be interpreted as indirect suggestive evidence. For instance, Mininni and Pouquet (2009) showed that *fast dissipation* takes place in 3D MHD turbulence. This phenomenon is consistent with the idea of fast reconnection, but naturally cannot be treated as any proof. Obviously, fast dissipation and fast magnetic reconnection are rather different physical processes, dealing with decrease of energy on the one hand and decrease of magnetic flux on the other.

Similarly, work by Galsgaard and Nordlund (1997) could also be considered as being in agreement with fast reconnection idea. The authors showed that in their simulations they could not produce highly twisted magnetic fields. These configurations are subject to kink instability and the instability can produce turbulence and induce reconnection. However, in view of many uncertainties of the numerical studies, this relation is unclear. In fact, with low resolution involved in the simulations the Reynolds numbers could not allow a turbulent inertial-range. It is more likely that numerical finding in Lapenta and Bettarini (2011) which showed that reconnecting magnetic

configurations spontaneously get chaotic and dissipate are related to LV99 reconnection. This connection is discussed in Lapenta and Lazarian (2012).

11.2 Interrelation of different concepts

The concept of turbulent magnetic field wandering is a well-known concept that was long adopted and widely used in the cosmic ray literature to explain observational evidence for the fast diffusion of cosmic rays perpendicular to the mean galactic magnetic field[11]. Although this concept existed in cosmic ray literature decades before the theory of turbulent reconnection was formulated, it is easy to understand that it is impossible to account for the magnetic field wandering if magnetic field lines do not reconnect. As we discussed, magnetic wandering arises from the Richardson dispersion process and implies continuous reconnection and changing of connectivity of magnetic field lines.

The concept of transport of heat by turbulent eddies in magnetized plasmas (Cho et al, 2002b; Maron et al, 2004; Lazarian, 2006) can only be understood within the paradigm of fast turbulent reconnection that allows mixing motions perpendicular to the local magnetic field. The same is applicable to the turbulent transport of metals in interstellar gas. Both phenomena are related to the reconnection diffusion. At scales smaller than the scale of injection scale, reconnection diffusion follows the superdiffusive law dictated by the Richardson dispersion, which on the scales larger than the injection scale, the diffusive behavior is restored.

At scales smaller than the injection scale the magnetic field wandering quantified in LV99 represents the Richardson dispersion in space. Last, but not the least, fast turbulent reconnection makes the GS95 theory of MHD turbulence self-consistent (LV99, see also Lazarian et al, 2015b). All in all, magnetic turbulence and turbulent reconnection are intrinsically related.

11.3 Relation to other Chapters of the volume

This review deals with turbulent reconnection in MHD regime and explains how 3D magnetic turbulence makes reconnection fast for both collisional and

[11] It was shown in Lazarian and Yan (2014) that the mathematical formulation of the field wandering has an error in the classical papers, but this does not diminish the importance of the idea. In fact, learning about the efficient diffusion perpendicular to the mean magnetic field by charged particles provided an important impetus for one of the authors of this review towards the idea of turbulent reconnection.

collisionless fluids[12] MHD reconnection in laminar regime is addressed in the contribution by Priest (this volume). An interesting overlap in terms of conclusions is that the 3D and 2D reconnection processes are very different. Plasma effects related to reconnection and their laboratory studies are covered by Yamada et al. (this volume). The corresponding Reynolds numbers of reconnecting plasma outflows is insufficient for observing the regime of turbulent reconnection, but corresponds well to the present day two fluid simulations. The fact that thickness of the reconnection layers in the experiments is comparable with the ion inertial length makes this experiments very relevant to magnetospheric reconnection (see Cassak & Fuselier; Petrukovich et al., Raymond et al. this volume). We hope that in future experiments the reconnection will be studied in the conditions closer to those that we discuss in the review and turbulent driving will be employed to test our predictions.

A case of interlaced, but not turbulent fields is considered by Parker & Rappazzo (this volume). In terms of turbulent reconnection, such configurations generating flares of reconnection may be important for inducing turbulence in the system.

Within turbulent reconnection the microphysics of individual local small scale reconnection events is not relevant for determining the global reconnection rate. However, many processes that accompany turbulent reconnection events, e.g. energization/acceleration of particles from the thermal pool do depend on the detailed microphysics, e.g. collisionless plasma physics (see Yamada et al.; Scudder et al., this volume), electric field at the separatrix of local reconnection events (Lapenta et al., this volume).

Turbulent reconnection theory that we described does not deal with complex radiative processes that frequently manifest the reconnection events observationally. Their effects are described in detail by Uzdensky (this volume). In the case of relativistic reconnection we have shown that the effects of compressibility can play an important role changing the reconnection rate. Similarly, heating and cooling of media considered by Uzdensky (this volume) is expected to affect the rate of turbulent reconnection through the density of the outflow. At the same time we do not expect the change of resistivity that is related to heating to affect the turbulent reconnection rates.

The closest in spirit review is that by Shibata and Takasao (this volume). Fractal structure is the accepted feature of turbulence and transition from laminar to fractal reconnection that the authors describe has the important overlap with the physical processes that we describe in this review. The authors, however, more focused on reconnection mediated by plasmoid generation, which may also be viewed as a complementary approach. As we discuss above we view tearing as a transient process that for systems of sufficiently high Reynolds numbers leads to turbulent reconnection. Unlike tearing, the

[12] Turbulence is known to make other processes, e.g. diffusion of passive impurities independent of microphysics of diffusion in hydro. Thus the theory of turbulent reconnection just adds to the list of the transport processes which turbulence makes universal, i.e. independent of the detailed physics at the micro level.

final stage of turbulent reconnection does not depend on plasma microphysics, but only on the level of turbulence.

We feel that the beauty of turbulent reconnection as opposed to other suggestions is that it makes magnetic reconnection fast independently of detailed properties of plasmas, making magnetic reconnection really universal. This corresponds both to the principal of parsimony and to observations that do not see much difference between the two media as far as the rate of magnetic reconnection is concerned. However, the detailed microphysics of reconnection should not be disregarded. While we claim that it may not determine the resulting reconnection rates within sufficiently turbulent medium, the microphysics is likely to be important to other processes that accompany magnetic reconnection. In addition, particular intensively studied systems like Earth magnetosphere as well as many cases of plasmas presented in laboratory devices the thickness of reconnection layers is comparable with the plasma scales, making plasma effects important for reconnection in these systems. Thus magnetic reconnection presents a multi-facet problem where different approaches can be complementary.

Acknowledgements AL acknowledges the NSF grant AST 1212096, a distinguished visitor PVE/CAPES appointment at the Physics Graduate Program of the Federal University of Rio Grande do Norte and thanks the INCT INEspao and Physics Graduate Program/UFRN for hospitality. Final work on the review were done in a stimulating atmosphere of Bochum University during the visit supported by the Humboldt Foundation. GK acknowledges support from FAPESP (grants no. 2013/04073-2 and 2013/18815-0). EMGDP: Brazilian agencies FAPESP (2013/10559-5) and CNPq (306598/2009-4). JC acknowledges support from the National Research Foundation of Korea (NRF-2013R1A1A2064475).

References

Alfvén H (1943) On the Existence of Electromagnetic-Hydrodynamic Waves. Arkiv for Astronomi 29:1–7

Armstrong JW, Rickett BJ, Spangler SR (1995) Electron density power spectrum in the local interstellar medium. The Astrophysical Journal443:209–221, DOI 10.1086/175515

Balbus SA, Hawley JF (1998) Instability, turbulence, and enhanced transport in accretion disks. Reviews of Modern Physics 70:1–53, DOI 10.1103/RevModPhys.70.1

Bale SD, Kellogg PJ, Mozer FS, Horbury TS, Reme H (2005) Measurement of the Electric Fluctuation Spectrum of Magnetohydrodynamic Turbulence. Physical Review Letters 94(21):215002, DOI 10.1103/PhysRevLett.94.215002, `physics/0503103`

Beckwith K, Stone JM (2011) A Second-order Godunov Method for Multi-dimensional Relativistic Magnetohydrodynamics. The Astrophysical Journal Supplement Series193:6, DOI 10.1088/0067-0049/193/1/6, `1101.3573`

Beresnyak A (2013) Comment on Perez et al [PRX 2, 041005 (2012), arXiv:1209.2011]. ArXiv e-prints `1301.7425`

Beresnyak A (2014) Reply to Comment on "Spectra of strong magnetohydrodynamic turbulence from high-resolution simulations". ArXiv e-prints `1410.0957`

Beresnyak A (2015) On the Parallel Spectrum in Magnetohydrodynamic Turbulence. The Astrophysical Journal Letters801:L9, DOI 10.1088/2041-8205/801/1/L9, `1407.2613`

Beresnyak A, Lazarian A (2008) Strong Imbalanced Turbulence. The Astrophysical Journal682:1070–1075, DOI 10.1086/589428, 0709.0554

Beresnyak A, Lazarian A (2010) Scaling Laws and Diffuse Locality of Balanced and Imbalanced Magnetohydrodynamic Turbulence. The Astrophysical Journal Letters722:L110–L113, DOI 10.1088/2041-8205/722/1/L110, 1002.2428

Beresnyak A, Lazarian A (2015) MHD Turbulence, Turbulent Dynamo and Applications. In: Lazarian A, de Gouveia Dal Pino EM, Melioli C (eds) Astrophysics and Space Science Library, Astrophysics and Space Science Library, vol 407, p 163, DOI 10.1007/978-3-662-44625-6_8, 1406.1185

Bhattacharjee A, Hameiri E (1986) Self-consistent dynamolike activity in turbulent plasmas. Physical Review Letters 57:206–209, DOI 10.1103/PhysRevLett.57.206

Biskamp D (2003) Magnetohydrodynamic Turbulence

Boldyrev S (2002) Kolmogorov-Burgers Model for Star-forming Turbulence. The Astrophysical Journal569:841–845, DOI 10.1086/339403, astro-ph/0108300

Boldyrev S (2005) On the Spectrum of Magnetohydrodynamic Turbulence. The Astrophysical Journal Letters626:L37–L40, DOI 10.1086/431649, astro-ph/0503053

Boldyrev S (2006) Spectrum of Magnetohydrodynamic Turbulence. Physical Review Letters 96(11):115002, DOI 10.1103/PhysRevLett.96.115002, astro-ph/0511290

Boozer AH (2012) Separation of magnetic field lines. Physics of Plasmas 19(11):112901, DOI 10.1063/1.4765352

Boozer AH (2013) Tokamak halo currents. Physics of Plasmas 20(8):082510, DOI 10.1063/1.4817742

Brandenburg A, Lazarian A (2013) Astrophysical Hydromagnetic Turbulence. Space Science Reviews178:163–200, DOI 10.1007/s11214-013-0009-3, 1307.5496

Browning P, Lazarian A (2013) Notes on Magnetohydrodynamics of Magnetic Reconnection in Turbulent Media. Space Science Reviews178:325–355, DOI 10.1007/s11214-013-0022-6

Brunetti G, Lazarian A (2011) Acceleration of primary and secondary particles in galaxy clusters by compressible MHD turbulence: from radio haloes to gamma-rays. Monthly Notices of the Royal Astronomical Society410:127–142, DOI 10.1111/j.1365-2966.2010.17457.x, 1008.0184

Burlaga LF, Lepping RP, Behannon KW, Klein LW, Neubauer FM (1982) Large-scale variations of the interplanetary magnetic field - Voyager 1 and 2 observations between 1-5 AU. Journal of Geophysical Research87:4345–4353, DOI 10.1029/JA087iA06p04345

Casanova D, Lazarian A, Santos-Lima R (2015) The Astrophysical Journal, submitted

Cerutti B, Werner GR, Uzdensky DA, Begelman MC (2013) Simulations of Particle Acceleration beyond the Classical Synchrotron Burnoff Limit in Magnetic Reconnection: An Explanation of the Crab Flares. The Astrophysical Journal770:147, DOI 10.1088/0004-637X/770/2/147, 1302.6247

Cerutti B, Werner GR, Uzdensky DA, Begelman MC (2014) Three-dimensional Relativistic Pair Plasma Reconnection with Radiative Feedback in the Crab Nebula. The Astrophysical Journal782:104, DOI 10.1088/0004-637X/782/2/104, 1311.2605

Chandran BDG (2005) AGN-driven Convection in Galaxy-Cluster Plasmas. The Astrophysical Journal632:809–820, DOI 10.1086/432596, astro-ph/0506096

Chandran BDG, Cowley SC, Morris M (2000) Magnetic Flux Accumulation at the Galactic Center and Its Implications for the Strength of the Pregalactic Magnetic Field. The Astrophysical Journal528:723–733, DOI 10.1086/308184

Chepurnov A, Lazarian A (2010) Extending the Big Power Law in the Sky with Turbulence Spectra from Wisconsin Hα Mapper Data. The Astrophysical Journal710:853–858, DOI 10.1088/0004-637X/710/1/853, 0905.4413

Chepurnov A, Lazarian A, Stanimirović S, Heiles C, Peek JEG (2010) Velocity Spectrum for H I at High Latitudes. The Astrophysical Journal714:1398–1406, DOI 10.1088/0004-637X/714/2/1398, astro-ph/0611462

Chepurnov A, Burkhart B, Lazarian A, Stanimirovic S (2015) The Turbulence Velocity Power Spectrum of Neutral Hydrogen in the Small Magellanic Cloud. ArXiv e-prints 1506.03448

Cho J (2005) Simulations of Relativistic Force-free Magnetohydrodynamic Turbulence. The Astrophysical Journal621:324–327, DOI 10.1086/427493, astro-ph/0408318

Cho J (2014) Properties of balanced and imbalanced relativistic alfvénic magnetohydrodynamic turbulence. Journal of Korean Physical Society 65:871–875, DOI 10.3938/jkps.65.871

Cho J, Lazarian A (2002) Compressible Sub-Alfvénic MHD Turbulence in Low- β Plasmas. Physical Review Letters 88(24):245001, DOI 10.1103/PhysRevLett.88.245001, astro-ph/0205282

Cho J, Lazarian A (2003) Compressible magnetohydrodynamic turbulence: mode coupling, scaling relations, anisotropy, viscosity-damped regime and astrophysical implications. Monthly Notices of the Royal Astronomical Society345:325–339, DOI 10.1046/j.1365-8711.2003.06941.x, astro-ph/0301062

Cho J, Lazarian A (2014) Imbalanced Relativistic Force-free Magnetohydrodynamic Turbulence. The Astrophysical Journal780:30, DOI 10.1088/0004-637X/780/1/30, 1312.6128

Cho J, Vishniac ET (2000) The Anisotropy of Magnetohydrodynamic Alfvénic Turbulence. The Astrophysical Journal539:273–282, DOI 10.1086/309213, astro-ph/0003403

Cho J, Lazarian A, Vishniac ET (2002a) Simulations of Magnetohydrodynamic Turbulence in a Strongly Magnetized Medium. The Astrophysical Journal564:291–301, DOI 10.1086/324186, astro-ph/0105235

Cho J, Lazarian A, Vishniac ET (2002b) Simulations of Magnetohydrodynamic Turbulence in a Strongly Magnetized Medium. The Astrophysical Journal564:291–301, DOI 10.1086/324186, astro-ph/0105235

Cho J, Lazarian A, Vishniac ET (2003) MHD Turbulence: Scaling Laws and Astrophysical Implications. In: Falgarone E, Passot T (eds) Turbulence and Magnetic Fields in Astrophysics, Lecture Notes in Physics, Berlin Springer Verlag, vol 614, pp 56–98, astro-ph/0205286

Ciaravella A, Raymond JC (2008) The Current Sheet Associated with the 2003 November 4 Coronal Mass Ejection: Density, Temperature, Thickness, and Line Width. The Astrophysical Journal686:1372–1382, DOI 10.1086/590655

de Gouveia Dal Pino EM, Kowal G (2015) Particle Acceleration by Magnetic Reconnection. In: Lazarian A, de Gouveia Dal Pino EM, Melioli C (eds) Astrophysics and Space Science Library, Astrophysics and Space Science Library, vol 407, p 373, DOI 10.1007/978-3-662-44625-6_13, 1302.4374

de Gouveia Dal Pino EM, Lazarian A (2005) Production of the large scale superluminal ejections of the microquasar GRS 1915+105 by violent magnetic reconnection. Astronomy & Astrophysics441:845–853, DOI 10.1051/0004-6361:20042590

de Gouveia Dal Pino EM, Kowal G, Kadowaki LHS, Piovezan P, Lazarian A (2010a) Magnetic Field Effects Near the Launching Region of Astrophysical Jets. International Journal of Modern Physics D 19:729–739, DOI 10.1142/S0218271810016920, 1002.4434

de Gouveia Dal Pino EM, Piovezan PP, Kadowaki LHS (2010b) The role of magnetic reconnection on jet/accretion disk systems. Astronomy & Astrophysics518:A5, DOI 10.1051/0004-6361/200913462, 1005.3067

de Gouveia Dal Pino EM, Leão MRM, Santos-Lima R, Guerrero G, Kowal G, Lazarian A (2012) Magnetic flux transport by turbulent reconnection in astrophysical flows. Physica Scripta86(1):018401, DOI 10.1088/0031-8949/86/01/018401, 1112.4871

de Gouveia Dal Pino EM, Kowal G, Lazarian A (2014) Fermi Acceleration in Magnetic Reconnection Sites. In: Pogorelov NV, Audit E, Zank GP (eds) 8th International Conference of Numerical Modeling of Space Plasma Flows (ASTRONUM 2013), Astronomical Society of the Pacific Conference Series, vol 488, p 8, 1401.4941

Diamond PH, Malkov M (2003) Dynamics of helicity transport and Taylor relaxation. Physics of Plasmas 10:2322–2329, DOI 10.1063/1.1576390

Dobler W, Haugen NE, Yousef TA, Brandenburg A (2003) Bottleneck effect in three-dimensional turbulence simulations. Physical Review E68(2):026304, DOI 10.1103/PhysRevE.68.026304, astro-ph/0303324

Drake JF (2001) Magnetic explosions in space. Nature410:525–526

Drake JF, Swisdak M, Che H, Shay MA (2006) Electron acceleration from contracting magnetic islands during reconnection. Nature443:553–556, DOI 10.1038/nature05116

Drake JF, Opher M, Swisdak M, Chamoun JN (2010) A Magnetic Reconnection Mechanism for the Generation of Anomalous Cosmic Rays. The Astrophysical Journal709:963–974, DOI 10.1088/0004-637X/709/2/963, 0911.3098

Drenkhahn G, Spruit HC (2002) Efficient acceleration and radiation in Poynting flux powered GRB outflows. Astronomy & Astrophysics391:1141–1153, DOI 10.1051/0004-6361:20020839, astro-ph/0202387

Drury LO (2012) First-order Fermi acceleration driven by magnetic reconnection. Monthly Notices of the Royal Astronomical Society422:2474–2476, DOI 10.1111/j.1365-2966.2012.20804.x, 1201.6612

Enßlin TA, Vogt C (2006) Magnetic turbulence in cool cores of galaxy clusters. Astronomy & Astrophysics453:447–458, DOI 10.1051/0004-6361:20053518, astro-ph/0505517

Eyink G, Vishniac E, Lalescu C, Aluie H, Kanov K, Bürger K, Burns R, Meneveau C, Szalay A (2013) Flux-freezing breakdown in high-conductivity magnetohydrodynamic turbulence. Nature497:466–469, DOI 10.1038/nature12128

Eyink GL (2014) Turbulent General Magnetic Reconnection. ArXiv e-prints 1412.2254

Eyink GL, Lazarian A, Vishniac ET (2011) Fast Magnetic Reconnection and Spontaneous Stochasticity. The Astrophysical Journal743:51, DOI 10.1088/0004-637X/743/1/51, 1103.1882

Fatuzzo M, Adams FC (2002) Enhancement of Ambipolar Diffusion Rates through Field Fluctuations. The Astrophysical Journal570:210–221, DOI 10.1086/339502, astro-ph/0201131

Ferrière KM (2001) The interstellar environment of our galaxy. Reviews of Modern Physics 73:1031–1066, DOI 10.1103/RevModPhys.73.1031, astro-ph/0106359

Galsgaard K, Nordlund Å (1997) Heating and activity of the solar corona. 3. Dynamics of a low beta plasma with three-dimensional null points. Journal of Geophysical Research102:231–248, DOI 10.1029/96JA02680

Galtier S, Banerjee S (2011) Exact Relation for Correlation Functions in Compressible Isothermal Turbulence. Physical Review Letters 107(13):134501, DOI 10.1103/PhysRevLett.107.134501, 1108.4529

Galtier S, Nazarenko SV, Newell AC, Pouquet A (2000) A weak turbulence theory for incompressible magnetohydrodynamics. Journal of Plasma Physics 63:447–488, DOI 10.1017/S0022377899008284, astro-ph/0008148

Galtier S, Nazarenko SV, Newell AC, Pouquet A (2002) Anisotropic Turbulence of Shear-Alfvén Waves. The Astrophysical Journal Letters564:L49–L52, DOI 10.1086/338791

Garrison D, Nguyen P (2015) Characterization of Relativistic MHD Turbulence. ArXiv e-prints 1501.06068

Gerrard CL, Hood AW (2003) Kink unstable coronal loops: current sheets, current saturation and magnetic reconnection. Solar Physics214:151–169, DOI 10.1023/A:1024053501326

Giannios D (2008) Prompt GRB emission from gradual energy dissipation. Astronomy & Astrophysics480:305–312, DOI 10.1051/0004-6361:20079085, 0711.2632

Giannios D (2010) UHECRs from magnetic reconnection in relativistic jets. Monthly Notices of the Royal Astronomical Society408:L46–L50, DOI 10.1111/j.1745-3933.2010.00925.x, 1007.1522

Giannios D, Spruit HC (2006) The role of kink instability in Poynting-flux dominated jets. Astronomy & Astrophysics450:887–898, DOI 10.1051/0004-6361:20054107, astro-ph/0601172

Goldreich P, Sridhar S (1995) Toward a theory of interstellar turbulence. 2: Strong alfvenic turbulence. The Astrophysical Journal438:763–775, DOI 10.1086/175121

Gosling JT (2007) Observations of Magnetic Reconnection in the Turbulent High-Speed Solar Wind. The Astrophysical Journal Letters671:L73–L76, DOI 10.1086/524842

Guo F, Liu YH, Daughton W, Li H (2015) Particle Acceleration and Plasma Dynamics during Magnetic Reconnection in the Magnetically Dominated Regime. The Astrophysical Journal806:167, DOI 10.1088/0004-637X/806/2/167, 1504.02193

Guo ZB, Diamond PH, Wang XG (2012) Magnetic Reconnection, Helicity Dynamics, and Hyper-diffusion. The Astrophysical Journal757:173, DOI 10.1088/0004-637X/757/2/173

Hameiri E, Bhattacharjee A (1987) Turbulent magnetic diffusion and magnetic field reversal. Physics of Fluids 30:1743–1755, DOI 10.1063/1.866241

Heitsch F, Zweibel EG (2003) Suppression of Fast Reconnection by Magnetic Shear. The Astrophysical Journal590:291–295, DOI 10.1086/375009

Heitsch F, Zweibel EG, Slyz AD, Devriendt JEG (2004) Magnetic Flux Transport in the ISM Through Turbulent Ambipolar Diffusion. Astrophysics and Space Science292:45–51, DOI 10.1023/B:ASTR.0000044999.25908.a5

Higashimori K, Hoshino M (2012) The relation between ion temperature anisotropy and formation of slow shocks in collisionless magnetic reconnection. Journal of Geophysical Research (Space Physics) 117:A01220, DOI 10.1029/2011JA016817, 1201.4213

Higdon JC (1984) Density fluctuations in the interstellar medium: Evidence for anisotropic magnetogasdynamic turbulence. I - Model and astrophysical sites. The Astrophysical Journal285:109–123, DOI 10.1086/162481

Hoshino M, Lyubarsky Y (2012) Relativistic Reconnection and Particle Acceleration. Space Science Reviews173:521–533, DOI 10.1007/s11214-012-9931-z

Inoue T, Asano K, Ioka K (2011) Three-dimensional Simulations of Magnetohydrodynamic Turbulence Behind Relativistic Shock Waves and Their Implications for Gamma-Ray Bursts. The Astrophysical Journal734:77, DOI 10.1088/0004-637X/734/2/77, 1011.6350

Iroshnikov PS (1964) Turbulence of a Conducting Fluid in a Strong Magnetic Field. Soviet Astronomy7:566

Jaroschek CH, Lesch H, Treumann RA (2004) Relativistic Kinetic Reconnection as the Possible Source Mechanism for High Variability and Flat Spectra in Extragalactic Radio Sources. The Astrophysical Journal Letters605:L9–L12, DOI 10.1086/420767

Kadowaki LHS, de Gouveia Dal Pino EM, Singh CB (2015) The Role of Fast Magnetic Reconnection on the Radio and Gamma-ray Emission from the Nuclear Regions of Microquasars and Low Luminosity AGNs. The Astrophysical Journal802:113, DOI 10.1088/0004-637X/802/2/113, 1410.3454

Karimabadi H, Lazarian A (2013) Magnetic reconnection in the presence of externally driven and self-generated turbulence. Physics of Plasmas 20(11):112,102, DOI 10.1063/1.4828395

Karimabadi H, Roytershteyn V, Vu HX, Omelchenko YA, Scudder J, Daughton W, Dimmock A, Nykyri K, Wan M, Sibeck D, Tatineni M, Majumdar A, Loring B, Geveci B (2014) The link between shocks, turbulence, and magnetic reconnection in collisionless plasmas. Physics of Plasmas 21(6):062308, DOI 10.1063/1.4882875

Khabarova O, Obridko V (2012) Puzzles of the Interplanetary Magnetic Field in the Inner Heliosphere. The Astrophysical Journal761:82, DOI 10.1088/0004-637X/761/2/82, 1204.6672

Khiali B, de Gouveia Dal Pino EM (2015) Very high energy neutrino emission from the core of low luminosity AGNs triggered by magnetic reconnection acceleration. ArXiv e-prints 1506.01063

Khiali B, de Gouveia Dal Pino EM, del Valle MV (2015a) A magnetic reconnection model for explaining the multiwavelength emission of the microquasars Cyg X-1 and Cyg X-3. Monthly Notices of the Royal Astronomical Society449:34–48, DOI 10.1093/mnras/stv248, 1406.5664

Khiali B, de Gouveia Dal Pino EM, Sol H (2015b) Particle Acceleration and Gamma-ray emission due to magnetic reconnection in the core region of radio galaxies. ArXiv e-prints 1504.07592

Kim Ej, Diamond PH (2001) On Turbulent Reconnection. The Astrophysical Journal556:1052–1065, DOI 10.1086/321628, astro-ph/0101161

Komissarov SS (2002) Time-dependent, force-free, degenerate electrodynamics. Monthly Notices of the Royal Astronomical Society336:759–766, DOI 10.1046/j.1365-8711.2002.05313.x, astro-ph/0202447

Kowal G, Lazarian A (2007) Scaling Relations of Compressible MHD Turbulence. The Astrophysical Journal Letters666:L69–L72, DOI 10.1086/521788, 0705.2464

Kowal G, Lazarian A (2010) Velocity Field of Compressible Magnetohydrodynamic Turbulence: Wavelet Decomposition and Mode Scalings. The Astrophysical Journal720:742–756, DOI 10.1088/0004-637X/720/1/742, 1003.3697

Kowal G, Lazarian A, Beresnyak A (2007) Density Fluctuations in MHD Turbulence: Spectra, Intermittency, and Topology. The Astrophysical Journal658:423–445, DOI 10.1086/511515, astro-ph/0608051

Kowal G, Lazarian A, Vishniac ET, Otmianowska-Mazur K (2009) Numerical Tests of Fast Reconnection in Weakly Stochastic Magnetic Fields. The Astrophysical Journal700:63–85, DOI 10.1088/0004-637X/700/1/63, 0903.2052

Kowal G, de Gouveia Dal Pino EM, Lazarian A (2011) Magnetohydrodynamic Simulations of Reconnection and Particle Acceleration: Three-dimensional Effects. The Astrophysical Journal735:102, DOI 10.1088/0004-637X/735/2/102, 1103.2984

Kowal G, Lazarian A, Vishniac ET, Otmianowska-Mazur K (2012) Reconnection studies under different types of turbulence driving. Nonlinear Processes in Geophysics 19:297–314, DOI 10.5194/npg-19-297-2012, 1203.2971

Kowal G, Falceta-Gon DA calves, Lazarian A, Vishniac ET (2015) Turbulence generated by reconnection. preprint

Kraichnan RH (1965) Inertial-Range Spectrum of Hydromagnetic Turbulence. Physics of Fluids 8:1385–1387, DOI 10.1063/1.1761412

Kritsuk AG, Norman ML, Padoan P, Wagner R (2007) The Statistics of Supersonic Isothermal Turbulence. The Astrophysical Journal665:416–431, DOI 10.1086/519443, 0704.3851

Kulpa-Dybeł K, Kowal G, Otmianowska-Mazur K, Lazarian A, Vishniac E (2010) Reconnection in weakly stochastic B-fields in 2D. Astronomy & Astrophysics514:A26, DOI 10.1051/0004-6361/200913218, 0909.1265

Kupiainen A (2003) Nondeterministic Dynamics and Turbulent Transport. Annales Henri Poincaré 4:713–726, DOI 10.1007/s00023-003-0957-3

Lalescu CC, Shi YK, Eyink GL, Drivas TD, Vishniac ET, Lazarian A (2015) Inertial-Range Reconnection in Magnetohydrodynamic Turbulence and in the Solar Wind. Physical Review Letters 115(2):025001, DOI 10.1103/PhysRevLett.115.025001, 1503.00509

Lapenta G (2008) Self-Feeding Turbulent Magnetic Reconnection on Macroscopic Scales. Physical Review Letters 100(23):235001, DOI 10.1103/PhysRevLett.100.235001, 0805.0426

Lapenta G, Bettarini L (2011) Spontaneous transition to a fast 3D turbulent reconnection regime. EPL (Europhysics Letters) 93:65,001, DOI 10.1209/0295-5075/93/65001, 1102.4791

Lapenta G, Lazarian A (2012) Achieving fast reconnection in resistive MHD models via turbulent means. Nonlinear Processes in Geophysics 19:251–263, DOI 10.5194/npg-19-251-2012, 1110.0089

Lazarian A (2005) Astrophysical Implications of Turbulent Reconnection: from cosmic rays to star formation. In: de Gouveia dal Pino EM, Lugones G, Lazarian A (eds) Magnetic Fields in the Universe: From Laboratory and Stars to Primordial Structures., American Institute of Physics Conference Series, vol 784, pp 42–53, DOI 10.1063/1.2077170, astro-ph/0505574

Lazarian A (2006) Enhancement and Suppression of Heat Transfer by MHD Turbulence. The Astrophysical Journal Letters645:L25–L28, DOI 10.1086/505796, astro-ph/0608045

Lazarian A (2009) Obtaining Spectra of Turbulent Velocity from Observations. Space Science Reviews143:357–385, DOI 10.1007/s11214-008-9460-y, 0811.0839

Lazarian A (2011) Fast Reconnection and Reconnection Diffusion: Implications for Star Formation. ArXiv e-prints 1111.0694

Lazarian A (2014) Reconnection Diffusion in Turbulent Fluids and Its Implications for Star Formation. Space Science Reviews181:1–59, DOI 10.1007/s11214-013-0031-5

Lazarian A, Beresnyak A (2006) Cosmic ray scattering in compressible turbulence. Monthly Notices of the Royal Astronomical Society373:1195–1202, DOI 10.1111/j.1365-2966.2006.11093.x, astro-ph/0606737

Lazarian A, Desiati P (2010) Magnetic Reconnection as the Cause of Cosmic Ray Excess from the Heliospheric Tail. The Astrophysical Journal722:188–196, DOI 10.1088/0004-637X/722/1/188, 1008.1981

Lazarian A, Medvedev MV (2015) preprint

Lazarian A, Opher M (2009) A Model of Acceleration of Anomalous Cosmic Rays by Reconnection in the Heliosheath. The Astrophysical Journal703:8–21, DOI 10.1088/0004-637X/703/1/8, 0905.1120

Lazarian A, Pogosyan D (2000) Velocity Modification of H I Power Spectrum. The Astrophysical Journal537:720–748, DOI 10.1086/309040, astro-ph/9901241

Lazarian A, Pogosyan D (2004) Velocity Modification of the Power Spectrum from an Absorbing Medium. The Astrophysical Journal616:943–965, DOI 10.1086/422462, astro-ph/0405461

Lazarian A, Pogosyan D (2006) Studying Turbulence Using Doppler-broadened Lines: Velocity Coordinate Spectrum. The Astrophysical Journal652:1348–1365, DOI 10.1086/508012, astro-ph/0511248

Lazarian A, Pogosyan D (2012) Statistical Description of Synchrotron Intensity Fluctuations: Studies of Astrophysical Magnetic Turbulence. The Astrophysical Journal747:5, DOI 10.1088/0004-637X/747/1/5, 1105.4617

Lazarian A, Vishniac ET (1999) Reconnection in a Weakly Stochastic Field. The Astrophysical Journal517:700–718, DOI 10.1086/307233, astro-ph/9811037

Lazarian A, Vishniac ET (2009) Model of Reconnection of Weakly Stochastic Magnetic Field and its Implications. In: Revista Mexicana de Astronomia y Astrofisica Conference Series, Revista Mexicana de Astronomia y Astrofisica, vol. 27, vol 36, pp 81–88, 0812.2019

Lazarian A, Yan H (2014) Superdiffusion of Cosmic Rays: Implications for Cosmic Ray Acceleration. The Astrophysical Journal784:38, DOI 10.1088/0004-637X/784/1/38, 1308.3244

Lazarian A, Petrosian V, Yan H, Cho J (2003) Physics of Gamma-Ray Bursts: Turbulence, Energy Transfer and Reconnection. ArXiv Astrophysics e-prints astro-ph/0301181

Lazarian A, Vishniac ET, Cho J (2004) Magnetic Field Structure and Stochastic Reconnection in a Partially Ionized Gas. The Astrophysical Journal603:180–197, DOI 10.1086/381383, physics/0311051

Lazarian A, Kowal G, de Gouveia dal Pino B (2012) Astrophysical Reconnection and Particle Acceleration. In: Pogorelov NV, Font JA, Audit E, Zank GP (eds) Numerical Modeling of Space Plasma Slows (ASTRONUM 2011), Astronomical Society of the Pacific Conference Series, vol 459, p 21, 1202.1559

Lazarian A, Eyink GL, Vishniac ET, Kowal G (2015a) Magnetic Reconnection in Astrophysical Environments. In: Lazarian A, de Gouveia Dal Pino EM, Melioli C (eds) Astrophysics and Space Science Library, Astrophysics and Space Science Library, vol 407, p 311, DOI 10.1007/978-3-662-44625-6_12, 1407.6356

Lazarian A, Eyink GL, Vishniac ET, Kowal G (2015b) Turbulent Reconnection and Its Implications. ArXiv e-prints 1502.01396

Lazarian A, Eyink GL, Vishniac ET, Kowal G (2015c) Turbulent Reconnection and Its Implications. ArXiv e-prints 1502.01396

Leão MRM, de Gouveia Dal Pino EM, Santos-Lima R, Lazarian A (2013) The Collapse of Turbulent Cores and Reconnection Diffusion. The Astrophysical Journal777:46, DOI 10.1088/0004-637X/777/1/46, 1209.1846

Leamon RJ, Smith CW, Ness NF, Matthaeus WH, Wong HK (1998) Observational constraints on the dynamics of the interplanetary magnetic field dissipation range. Journal of Geophysical Research103:4775, DOI 10.1029/97JA03394

Lithwick Y, Goldreich P (2001) Compressible Magnetohydrodynamic Turbulence in Interstellar Plasmas. The Astrophysical Journal562:279–296, DOI 10.1086/323470, astro-ph/0106425

Litvinenko YE (1996) Particle Acceleration in Reconnecting Current Sheets with a Nonzero Magnetic Field. The Astrophysical Journal462:997, DOI 10.1086/177213

Loureiro NF, Schekochihin AA, Cowley SC (2007) Instability of current sheets and formation of plasmoid chains. Physics of Plasmas 14(10):100,703, DOI 10.1063/1.2783986, astro-ph/0703631

Loureiro NF, Uzdensky DA, Schekochihin AA, Cowley SC, Yousef TA (2009) Turbulent magnetic reconnection in two dimensions. Monthly Notices of the Royal Astronomical Society399:L146–L150, DOI 10.1111/j.1745-3933.2009.00742.x, 0904.0823

Lyutikov M, Lazarian A (2013) Topics in Microphysics of Relativistic Plasmas. Space Science Reviews178:459–481, DOI 10.1007/s11214-013-9989-2, 1305.3838

Maron J, Goldreich P (2001) Simulations of Incompressible Magnetohydrodynamic Turbulence. The Astrophysical Journal554:1175–1196, DOI 10.1086/321413, astro-ph/0012491

Maron J, Chandran BD, Blackman E (2004) Divergence of Neighboring Magnetic-Field Lines and Fast-Particle Diffusion in Strong Magnetohydrodynamic Turbulence, with Application to Thermal Conduction in Galaxy Clusters. Physical Review Letters 92(4):045001, DOI 10.1103/PhysRevLett.92.045001, astro-ph/0303217

Mason J, Cattaneo F, Boldyrev S (2006) Dynamic Alignment in Driven Magnetohydrodynamic Turbulence. Physical Review Letters 97(25):255002, DOI 10.1103/PhysRevLett.97.255002, astro-ph/0602382

Mason J, Cattaneo F, Boldyrev S (2008) Numerical measurements of the spectrum in magnetohydrodynamic turbulence. Physical Review E77(3):036403, DOI 10.1103/PhysRevE.77.036403, 0706.2003

Matthaeus WH, Lamkin SL (1985) Rapid magnetic reconnection caused by finite amplitude fluctuations. Physics of Fluids 28:303–307, DOI 10.1063/1.865147

Matthaeus WH, Lamkin SL (1986) Turbulent magnetic reconnection. Physics of Fluids 29:2513–2534, DOI 10.1063/1.866004

Matthaeus WH, Montgomery DC, Goldstein ML (1983) Turbulent generation of outward-traveling interplanetary Alfvenic fluctuations. Physical Review Letters 51:1484–1487, DOI 10.1103/PhysRevLett.51.1484

McKinney JC, Uzdensky DA (2012) A reconnection switch to trigger gamma-ray burst jet dissipation. Monthly Notices of the Royal Astronomical Society419:573–607, DOI 10.1111/j.1365-2966.2011.19721.x, 1011.1904

Meier DL (2012) Black Hole Astrophysics: The Engine Paradigm

Merloni A, Heinz S, di Matteo T (2003) A Fundamental Plane of black hole activity. Monthly Notices of the Royal Astronomical Society345:1057–1076, DOI 10.1046/j.1365-2966.2003.07017.x, astro-ph/0305261

Miesch MS, Matthaeus WH, Brandenburg A, Petrosyan A, Pouquet A, Cambon C, Jenko F, Uzdensky D, Stone J, Tobias S, Toomre J, Velli M (2015) Large-Eddy Simulations of Magnetohydrodynamic Turbulence in Astrophysics and Space Physics. ArXiv e-prints 1505.01808

Mininni PD, Pouquet A (2009) Finite dissipation and intermittency in magnetohydrodynamics. Physical Review E80(2):025401, DOI 10.1103/PhysRevE.80.025401, 0903.3265

Mizuno Y, Singh C, de Gouveia Dal Pino EM (2015) in preparation. preprint
Montgomery D, Turner L (1981) Anisotropic magnetohydrodynamic turbulence in a strong external magnetic field. Physics of Fluids 24:825–831, DOI 10.1063/1.863455
Müller WC, Grappin R (2005) Spectral Energy Dynamics in Magnetohydrodynamic Turbulence. Physical Review Letters 95(11):114502, DOI 10.1103/PhysRevLett.95.114502, physics/0509019
Narayan R, Medvedev MV (2003) Self-similar hot accretion on to a spinning neutron star: matching the outer boundary conditions. Monthly Notices of the Royal Astronomical Society343:1007–1012, DOI 10.1046/j.1365-8711.2003.06747.x, astro-ph/0305002
Narayan R, Yi I (1995) Advection-dominated Accretion: Underfed Black Holes and Neutron Stars. The Astrophysical Journal452:710, DOI 10.1086/176343, astro-ph/9411059
Ng CS, Bhattacharjee A (1996) Interaction of Shear-Alfven Wave Packets: Implication for Weak Magnetohydrodynamic Turbulence in Astrophysical Plasmas. The Astrophysical Journal465:845, DOI 10.1086/177468
Norman CA, Ferrara A (1996) The Turbulent Interstellar Medium: Generalizing to a Scale-dependent Phase Continuum. The Astrophysical Journal467:280, DOI 10.1086/177603, astro-ph/9602146
Oishi JS, Mac Low MM, Collins DC, Tamura M (2015) Self-generated turbulence in magnetic reconnection. ArXiv e-prints 1505.04653
Padoan P, Juvela M, Kritsuk A, Norman ML (2006) The Power Spectrum of Supersonic Turbulence in Perseus. The Astrophysical Journal Letters653:L125–L128, DOI 10.1086/510620, astro-ph/0611248
Padoan P, Kritsuk AG, Lunttila T, Juvela M, Nordlund A, Norman ML, Ustyugov SD (2010) MHD Turbulence In Star-Forming Clouds. In: Bertin G, de Luca F, Lodato G, Pozzoli R, Romé M (eds) American Institute of Physics Conference Series, American Institute of Physics Conference Series, vol 1242, pp 219–230, DOI 10.1063/1.3460128
Papadopoulos PP, Thi WF, Miniati F, Viti S (2011) Extreme cosmic ray dominated regions: a new paradigm for high star formation density events in the Universe. Monthly Notices of the Royal Astronomical Society414:1705–1714, DOI 10.1111/j.1365-2966.2011.18504.x, 1009.2496
Parker EN (1957) Sweet's Mechanism for Merging Magnetic Fields in Conducting Fluids. Journal of Geophysical Research62:509–520, DOI 10.1029/JZ062i004p00509
Parker EN (1979) Cosmical magnetic fields: Their origin and their activity
Perez JC, Mason J, Boldyrev S, Cattaneo F (2012) On the Energy Spectrum of Strong Magnetohydrodynamic Turbulence. Physical Review X 2(4):041005, DOI 10.1103/PhysRevX.2.041005, 1209.2011
Radice D, Rezzolla L (2013) Universality and Intermittency in Relativistic Turbulent Flows of a Hot Plasma. The Astrophysical Journal Letters766:L10, DOI 10.1088/2041-8205/766/1/L10, 1209.2936
Rechester AB, Rosenbluth MN (1978) Electron heat transport in a Tokamak with destroyed magnetic surfaces. Physical Review Letters 40:38–41, DOI 10.1103/PhysRevLett.40.38
Rocha da Silva G, Falceta-Gonçalves D, Kowal G, de Gouveia Dal Pino EM (2015) Ambient magnetic field amplification in shock fronts of relativistic jets: an application to GRB afterglows. Monthly Notices of the Royal Astronomical Society446:104–119, DOI 10.1093/mnras/stu2104, 1410.2776
Santos-Lima R, Lazarian A, de Gouveia Dal Pino EM, Cho J (2010) Diffusion of Magnetic Field and Removal of Magnetic Flux from Clouds Via Turbulent Reconnection. The Astrophysical Journal714:442–461, DOI 10.1088/0004-637X/714/1/442, 0910.1117
Santos-Lima R, de Gouveia Dal Pino EM, Lazarian A (2012) The Role of Turbulent Magnetic Reconnection in the Formation of Rotationally Supported Protostellar Disks. The Astrophysical Journal747:21, DOI 10.1088/0004-637X/747/1/21, 1109.3716
Santos-Lima R, de Gouveia Dal Pino EM, Lazarian A (2013) Disc formation in turbulent cloud cores: is magnetic flux loss necessary to stop the magnetic braking catastrophe or

not? Monthly Notices of the Royal Astronomical Society429:3371–3378, DOI 10.1093/mnras/sts597, 1211.1059

Schekochihin AA, Cowley SC, Dorland W, Hammett GW, Howes GG, Quataert E, Tatsuno T (2009) Astrophysical Gyrokinetics: Kinetic and Fluid Turbulent Cascades in Magnetized Weakly Collisional Plasmas. The Astrophysical Journal Supplement Series182:310–377, DOI 10.1088/0067-0049/182/1/310, 0704.0044

Servidio S, Matthaeus WH, Shay MA, Dmitruk P, Cassak PA, Wan M (2010) Statistics of magnetic reconnection in two-dimensional magnetohydrodynamic turbulence. Physics of Plasmas 17(3):032315, DOI 10.1063/1.3368798

Shay MA, Drake JF, Denton RE, Biskamp D (1998) Structure of the dissipation region during collisionless magnetic reconnection. Journal of Geophysical Research103:9165–9176, DOI 10.1029/97JA03528

Shay MA, Drake JF, Swisdak M, Rogers BN (2004) The scaling of embedded collisionless reconnection. Physics of Plasmas 11:2199–2213, DOI 10.1063/1.1705650

She ZS, Leveque E (1994) Universal scaling laws in fully developed turbulence. Physical Review Letters 72:336–339, DOI 10.1103/PhysRevLett.72.336

Shebalin JV, Matthaeus WH, Montgomery D (1983) Anisotropy in MHD turbulence due to a mean magnetic field. Journal of Plasma Physics 29:525–547, DOI 10.1017/S0022377800000933

Shibata K, Tanuma S (2001) Plasmoid-induced-reconnection and fractal reconnection. Earth, Planets, and Space 53:473–482, astro-ph/0101008

Shu FH (1983) Ambipolar diffusion in self-gravitating isothermal layers. The Astrophysical Journal273:202–213, DOI 10.1086/161359

Singh CB, de Gouveia Dal Pino EM, Kadowaki LHS (2015) On the Role of Fast Magnetic Reconnection in Accreting Black Hole Sources. The Astrophysical Journal Letters799:L20, DOI 10.1088/2041-8205/799/2/L20, 1411.0883

Sironi L, Spitkovsky A (2014) Relativistic Reconnection: An Efficient Source of Nonthermal Particles. The Astrophysical Journal Letters783:L21, DOI 10.1088/2041-8205/783/1/L21, 1401.5471

Stanimirović S, Lazarian A (2001) Velocity and Density Spectra of the Small Magellanic Cloud. The Astrophysical Journal Letters551:L53–L56, DOI 10.1086/319837, astro-ph/0102191

Strauss HR (1986) Hyper-resistivity produced by tearing mode turbulence. Physics of Fluids 29:3668–3671, DOI 10.1063/1.865798

Subramanian K, Shukurov A, Haugen NEL (2006) Evolving turbulence and magnetic fields in galaxy clusters. Monthly Notices of the Royal Astronomical Society366:1437–1454, DOI 10.1111/j.1365-2966.2006.09918.x, astro-ph/0505144

Sweet PA (1958) The topology of force-free magnetic fields. The Observatory 78:30–32

Sych R, Nakariakov VM, Karlicky M, Anfinogentov S (2009) Relationship between wave processes in sunspots and quasi-periodic pulsations in active region flares. Astronomy & Astrophysics505:791–799, DOI 10.1051/0004-6361/200912132, 1005.3594

Syrovatskii SI (1981) Pinch sheets and reconnection in astrophysics. Annual Review of Astronomy & Astrophysics19:163–229, DOI 10.1146/annurev.aa.19.090181.001115

Sytine IV, Porter DH, Woodward PR, Hodson SW, Winkler KH (2000) Convergence Tests for the Piecewise Parabolic Method and Navier-Stokes Solutions for Homogeneous Compressible Turbulence. Journal of Computational Physics 158:225–238, DOI 10.1006/jcph.1999.6416

Takamoto M, Inoue T (2011) A New Numerical Scheme for Resistive Relativistic Magnetohydrodynamics Using Method of Characteristics. The Astrophysical Journal735:113, DOI 10.1088/0004-637X/735/2/113, 1105.5683

Takamoto M, Inoue T, Lazarian A (2015) Turbulent relativistic reconnection. The Astrophysical Journal, submitted

Tennekes H, Lumley JL (1972) First Course in Turbulence

Thompson C, Blaes O (1998) Magnetohydrodynamics in the extreme relativistic limit. Physical Review D57:3219–3234, DOI 10.1103/PhysRevD.57.3219

Uzdensky DA, Spitkovsky A (2014) Physical Conditions in the Reconnection Layer in Pulsar Magnetospheres. The Astrophysical Journal780:3, DOI 10.1088/0004-637X/780/1/3, 1210.3346

Uzdensky DA, Loureiro NF, Schekochihin AA (2010) Fast Magnetic Reconnection in the Plasmoid-Dominated Regime. Physical Review Letters 105(23):235002, DOI 10.1103/PhysRevLett.105.235002, 1008.3330

Vishniac ET, Lazarian A (1999) Reconnection in the Interstellar Medium. The Astrophysical Journal511:193–203, DOI 10.1086/306643, astro-ph/9712067

Vishniac ET, Pillsworth S, Eyink G, Kowal G, Lazarian A, Murray S (2012) Reconnection current sheet structure in a turbulent medium. Nonlinear Processes in Geophysics 19:605–610, DOI 10.5194/npg-19-605-2012

Vogt C, Enßlin TA (2005) A Bayesian view on Faraday rotation maps Seeing the magnetic power spectra in galaxy clusters. Astronomy & Astrophysics434:67–76, DOI 10.1051/0004-6361:20041839, astro-ph/0501211

Watson PG, Oughton S, Craig IJD (2007) The impact of small-scale turbulence on laminar magnetic reconnection. Physics of Plasmas 14(3):032301, DOI 10.1063/1.2458595

Werner GR, Uzdensky DA, Cerutti B, Nalewajko K, Begelman MC (2014) The extent of power-law energy spectra in collisionless relativistic magnetic reconnection in pair plasmas. ArXiv e-prints 1409.8262

Xu S, Yan H, Lazarian A (2015) Damping of MHD turbulence in partially ionized plasma: implications for cosmic ray propagation. ArXiv e-prints 1506.05585

Yamada M, Kulsrud R, Ji H (2010) Magnetic reconnection. Reviews of Modern Physics 82:603–664, DOI 10.1103/RevModPhys.82.603

Zenitani S, Hoshino M (2001) The Generation of Nonthermal Particles in the Relativistic Magnetic Reconnection of Pair Plasmas. The Astrophysical Journal Letters562:L63–L66, DOI 10.1086/337972, 1402.7139

Zenitani S, Hoshino M (2008) The Role of the Guide Field in Relativistic Pair Plasma Reconnection. The Astrophysical Journal677:530–544, DOI 10.1086/528708, 0712.2016

Zenitani S, Hesse M, Klimas A (2009) Two-Fluid Magnetohydrodynamic Simulations of Relativistic Magnetic Reconnection. The Astrophysical Journal696:1385–1401, DOI 10.1088/0004-637X/696/2/1385, 0902.2074

Zhang B, Yan H (2011) The Internal-collision-induced Magnetic Reconnection and Turbulence (ICMART) Model of Gamma-ray Bursts. The Astrophysical Journal726:90, DOI 10.1088/0004-637X/726/2/90, 1011.1197

Zhang W, MacFadyen A, Wang P (2009) Three-Dimensional Relativistic Magnetohydrodynamic Simulations of the Kelvin-Helmholtz Instability: Magnetic Field Amplification by a Turbulent Dynamo. The Astrophysical Journal Letters692:L40–L44, DOI 10.1088/0004-637X/692/1/L40, 0811.3638

Zrake J, MacFadyen AI (2012) Numerical Simulations of Driven Relativistic Magnetohydrodynamic Turbulence. The Astrophysical Journal744:32, DOI 10.1088/0004-637X/744/1/32, 1108.1991

Zrake J, MacFadyen AI (2013) Spectral and Intermittency Properties of Relativistic Turbulence. The Astrophysical Journal Letters763:L12, DOI 10.1088/2041-8205/763/1/L12, 1210.4066

Zweibel EG (2002) Ambipolar Drift in a Turbulent Medium. The Astrophysical Journal567:962–970, DOI 10.1086/338682, astro-ph/0107462